End-of-degree project

Chemical Engineering Degree

Acid mine drainage treatment by nanofiltration membranes: impact of aluminium and iron concentration on membrane performance.

Dissertation

Autor: Bartomeu Servera Salas
Director: Oriol Gibert Agulló

Convocatòria: 01/2017

Escola Tècnica Superior
d'Enginyeria Industrial de Barcelona

ABSTRACT

The purpose of this study is to evaluate the rejection of different elements in acid mine drainage (AMD), specifically metals, by means of nanofiltration (NF) membranes.

AMD is characterised by its high acidity and high concentration of metals and sulphate. These aspects make AMD treatment a point of interest for industry and society. The main reasons for that are that being able to properly treat AMD and separate the different metals dissolved allows its recovery and reuse. Furthermore, proper treatment via NF increases water quality, as it decreases the concentration of dissolved metals, diminishing the effect they have on animals and plants when discharged into the environment.

Experiments were carried out in a laboratory-scale plant, based on a flat sheet membrane with recirculation of permeate and concentrate to the feed tank. A total of 9 experiments were designed, in order to study rejection of different species varying pH solution and concentration of aluminium or iron. The solutions were prepared to resemble AMD, including different metals (aluminium, zinc, copper…) and rare earth elements (REE) (lanthanum, neodynium…). Sample composition was analysed via ICP by the Institut de Diagnosi Ambiental i Estudis d'Aigüa (IDAEA) of the Consejo Superior de Investigaciones Científicas (CSIC).

After obtaining the rejection, data were modelled using the Solution-Diffusion-Film-Model, plotting dominant salt and trace ion rejection depending on the trans-membrane flux. This model also allowed permeability of single trace ions to be calculated, comparing experimental and theoretical values.

The results obtained show that addition of metals in the solution affect rejection of the species in the solution, as sulphate forms complexes with metal ions. As iron and aluminium concentrations increased, rejection was generally increased. This also supports the theory that divalent ions show higher rejection than monovalent ions.

Finally, experimental costs and environmental impact were addressed.

TABLE OF CONTENTS

1 GLOSSARY

AMD: Acid mine drainage

REE: Rare earth elements

REY: Rare earth elements and yttrium

ICP: Inductively coupled plasma

IEP: Iso-electric point

NF: Nanofiltration

RO: Reverse osmosis

UF: Ultrafiltration

SWM: Spiral-wound module

MWCO: Molecular-weight cutoffs

PVC: Polyvinyl chloride

CA: Cellulose acetate

CFV: Cross flow velocity

TMP: Trans-membrane pressure

K_w: Membrane permeability

J_v: Trans-membrane flux

SDFM: Solution-Diffusion-Film-Model

2 ACID MINE DRAINAGE

Acid mine drainage (AMD) is a term used to describe the residual waters that origin from any activity that disturbs mineralized materials, which are generally related to the mining industry. This naturally occurring process results in a waste characterised by its high acidity and significant concentrations of sulphates and other various metals, which, if left untreated, can result in a far-reaching pollution problem to both the soil and groundwaters.

Although there are a lot of factors involved in the formation of AMD, the main cause is the oxidation of sulphide minerals such as pyrite (FeS_2). This phenomenon takes place when these materials are exposed to oxygen, water and microorganisms and involves chemical and biological reactions, which vary depending on the enviromental conditions.

Sulphide minerals are formed under reducing conditions in the absence of oxygen and become unstable when exposed to atmospheric oxygen or oxygenated waters, due to excavations or other earth moving processes, causing their oxidation.

The chemical process behind the constitution of AMD has various steps, which will be exemplified taking pyrite as the sulphide mineral. The first step is the oxidation, resulting in ferrous ion and sulphates:

$$2FeS_2 + 7O_2 + H_2O \rightarrow Fe^{2+} + 4SO_4^{2-} + 2H^+ \quad (1)$$

In order for the reaction to progress, it needs an environment rich in oxygen and pH to be greater than 3.5- causing the ferrous ion formed to be oxidized to ferric ion:

$$4Fe^{2+} + O_2 + 4H^+ \leftrightarrow 4Fe^{3+} + 2H_2O \quad (2)$$

In conditions of low oxygen this reaction will not take place until pH reaches 8.5.

This reaction is the step that limits the rate at which the oxidation occurs and its speed may be severely altered depending on the conditions given. Furthermore, at pH between 2.3 and 3.5 the ferric ion precipitates:

$$Fe^{3+} + 3H_2O \leftrightarrow Fe(OH)_3 \downarrow + 3H^+ \quad (3)$$

If pH is lower than 2, hydroxides are not stable and the ferric ion remains in solution which may be utilized to oxidize additional pyrite:

$$FeS_2 + 14Fe^{3+} + 8H_2O \rightarrow 15Fe^{2+} + 2SO_4^{2-} + 16H^+ \quad (4)$$

In this last case, it is acknowledged that Fe^{3+} results in a more potent oxidant as oxygen, becoming the dominant reaction.

On a biological level the presence of the *Thiobacilus ferroxidans* bacteria significantly accelerates the process.[1]

2.1 IBERIAN PYRITE BELT

In Spain, this whole process was profoundly studied in the Iberian Pyrite Belt (IPB), a vast area located in the south of the peninsula, notorious for its non ferrous metal reserves resulting in a significant mining activity since the eighth century.

The waters of the rivers studied showed already highly acidic pH values, and metal contents were in the order of hundred to a few thousand of mg/L, although data suggested a highly variable nature of the conditions. The composition of the waters showed an extreme concentration of sulphate, as well as other different metals such as Fe, Al, Mg, Zn, Cu and Mn. There were also traces of As, Cd, Co, Ni, Pb and unusually high concentration of U and Th.

Parameter	Units	Acid mine drainage		Acidic mine pit lakes	
		Average [a]	Extreme case [b]	Average [c]	Extreme case [d]
pH	S.U.	2.7	0.82	2,6	1.2
T	ºC	21	16.5	23	24
EC	mS/cm	7.9	-	5.3	55.6
Eh	m	627	625	782	584
DO	mg/L	3.8	-	7,6	0
DO	% sat.	42	-	93	0
SO_4	mg/L	7.460	134.200	4.000	41.900
Na	mg/L	32	37	31	78
K	mg/L	3	130	2	12
Mg	mg/L	414	3.036	357	1.957
Ca	mg/L	162	137	180	286
Fet	mg/L	1.494	74,215 (1)	332	36.675
Fe(II)	mg/L	801	40,600 (2)	15	32.500
Fe(III)	mg/L	476	28,630 (2)	312	3.950
Al	mg/L	386	7.556	123	1.919
Mn	mg/L	37	38	34	128
Cu	mg/L	64	1.945	20	1.350
Zn	mg/L	169	1.096	31	6.670
As	µg/L	2.123	303	91	158.730
Cd	µg/L	490	13.759	102	18.020
Co	µg/L	3.413	2.447	1.100	18.689
Cr	µg/L	118	52	38	1.295
Ni	µg/L	1.063	3.220	656	5.214
Pb	µg/L	61	108	122	5.402
Th	µg/L	23	376	6	-
Tl	µg/L	27	2.683	4	-
U	µg/L	64	981	7	-
V	µg/L	65	6.756	27	-

Table 1 Average chemical composition of 62 AMD waters from 25 mines of the Iberian Pyrite Belt [2]

Another problem of AMD may be the occurrence of evaporative sulphate salts. In the margins of acidic effluents, and also directly from mining sites, soluble metal sulphates are found in solid form, revealing, amongst other metals, very high concentrations of Cu and Zn, which can get re-dissolved during rainstorms, deriving in the incorporation of toxic metals to the rivers.[2]

2.2 PRESENT TREATMENT TECHNOLOGIES

As it has already been mentioned before, appropriate treatment of AMD is definitely required for various reasons, the most important being the threat it represents to the health of humans, animals and plants due to the presence of heavy metals and low pH

of the waters. Although it is not known the exact effect of the exposure on humans, in plants and animals, mainly aquatic organisms, it causes cellular damage and can severely affect their growth, reproduction or physiology, sometimes resulting lethal.

Some AMD also contain Rare Earth Elements and Yttrium (REY), which have many different industrial applications and therefore their recovery is of interest.[3]

When it comes to treating the waters, a first step is limiting the exposure of pyritic materials to water and oxygen, if possible, minimising the formation of acidic products.

One of the most extended techniques applied in AMD treatment is selective precipitation, accomplished by adding alkaline reagents to increase pH and precipitate the dissolved metals as hydroxides. Although it provides effective remediation, this process has high operational costs and it generates substantial amounts of sludge that require proper disposal. Additionally, selective extraction is very difficult and additional treatment may be needed in order to recover and reuse heavy metals. [4]

Another approach that has reported favorable results is selective adsorption, implemented with nanomaterials, in order to achieve a large surface area of adsorption and small diffusion resistance, to minimise the loss of adsorption rate due to intraparticle diffusion. Materials used have successfully been regenerated and used multiple times before a significant decrease in adsorption rate was noted. [1]

Processes relying on ion exchange have also been studied, providing a simpler resolution to the issue, offering high selectivity to the removal of certain metals such as lead.[1]

Finally membrane separation processes are also being explored as a reliable alternative, granting a high rejection rate based on pressure driven separation. This method relies on a thin membrane that allows selective mass transport of solutes and solvants through it. The rate of transfer is controlled by pressure. [5]

Membrane separation has gained recognition keeping high metal rejection rates at a lower cost compared to traditional processes. Nanofiltration (NF) is included in this type of treatments, and it is one of the newer techniques where a lot of research has been done, since its results have been successful in water treatment.[1]

3 MEMBRANE TECHNOLOGY

Membranes have gained a lot of attention in the chemical engineering field in the last decades. This is mainly due to the wide range of applications, including water treatment, allowing a greater removal of substances than other methods thus obtaining a higher quality of treated water.

Membranes are considered as a thin semipermeable sheet, usually made of biological, synthetic or polymeric materials, that acts as a selective barrier. This is the key property that these methods capitalise on, as it allows certain components of the dissolution to permeate the membrane freely while impeding the permeation of other components. A feed-stream, containing a solute and a solvent, is forced through the membrane, which then is divided into two different streams, the permeate, which passed through the membrane and presents solute and solvent in lower concentrations compared to the feed-stream, and the concentrate, which is the stream rejected by the membrane, containing solute and solvent in higher concentrations than the entry current.

Although the principle of operation is reasonably straightforward, there are many/several parameters to take into consideration. Factors such as pressure, pH and temperature can directly affect the membrane performance. Thus, controlling them properly is crucial to obtain the maximum separation of the desired component and minimise the degradation of the membrane.[6]

3.1 MEMBRANE OPERATIONS

Membranes can be classified depending on the driving force of the operation. According to this classification, there are four big groups. Some membranes operate based on concentration gradient, such as dialysis, there are also operation based on and electric potential gradient, such as electrodialysis, temperature gradient, such as membrane distillation, and pressure gradient, as NF. From now on, this project will be focused in membranes that operate based on pressure.

The main pressure driven operations are microfiltration (MF), ultrafiltration (UF), reverse osmosis (RO), and NF membranes. MF membranes have the largest pore size and typically reject large particles and various microorganisms. UF membranes have smaller pores than MF membranes and, therefore, in addition to large particles and microorganisms, they can reject bacteria and soluble macromolecules such as proteins. RO membranes are effectively non-porous and, therefore, exclude particles and even many low molar mass species such as salt ions, organics, etc. NF membranes exhibit performance between RO and UF membranes.

Composition wise, all the mentioned membranes are synthetic organic polymers. MF and UF membranes are often made from the same materials, but prepared under different conditions so that different pore sizes are produced. Typical MF and UF polymers include polysulphone, polyacrylonitrile and polyacrylonitrile-polyvinyl chloride copolymers. MF membranes also include cellulose, acetate-cellulose, nitrate blends,

nylons, and polytetrafluoroethylene. RO membranes are typically either cellulose acetate or polysulphone coated with aromatic polyamides. NF membranes are made from cellulose acetate blends or polyamide composites like the RO membranes, or they could be modified forms of UF membranes such as sulphonated polysulphone.[7]

Table 2 shows a comparison between the different methods, specifying pore size and usual materials.

Membrane	Reverse osmosis (RO)	Nanofiltration (NF)	Ultrafiltration (UF)	Microfiltration (MF)
	Asymmetric	Asymmetric	Asymmetric	Asymmetric symmetric
Thin film thickness	1 micron 150 micron	1 micron 150 micron	1 micron 150–250 micron	1–150 micron
Rejection	High and low molecular weight compounds, NaCl, glucose, amino acids	High molecular weight compounds, mono-, di- and oligosaccharides, polyvalent ions	Macromolecules, proteins, polysaccharides, vira	Particles, clay, bacteria
Membrane materials[1]	Cellulose acetate (CA) thin film	CA, thin film	Ceramic, polysulfonic (PS), poly vinylidene flouride (PVDF), CA, thin film	Ceramic, PS, PVDF, CA
Pore size	<0.002 micron	<0.002 micron	0.02–0.2 micron	0.02–4 microns
Module configuration[2]	Tubular, spiral wound, plate-and-frame	Tubular spiral wound, plate-and-frame	Tubular hollow fiber spiral wound, plate-and-frame	Tubular, hollow fiber
Operating pressure	15–150 bar	5–35 bar	1-10 bar	<2 bar

Table 2 Comparison between the different pressure driven separation methods [5]

The theoretical base of pressure driven separation is based on the following equation:

$$J_i = k \cdot \Delta P \qquad (5)$$

which expresses the trans-membrane flux of solution, J_i, as a function of the pressure difference across the membrane Δp, and the permeability, k, which is the rate of passive diffusion of molecules through the membrane. [6]

3.2 TYPES OF MEMBRANES

Different types of membranes can be classified depending on its structure or its separation principle.

- Isotropic membranes.
  - Porous. The membrane contains pores usually contained in a range of sizes, depending on the technique of separation used. The filtration is based on particle size. More specifically, there are macroporous membranes (used in MF), mesoporous (used in UF) and microporous (used in NF). In order to achieve high selectivity, pores in the membrane need to be relatively smaller than the particles in the solution. Chemical and thermal stability are significant factors to consider when selecting porous materials because temperature and concentration affects selectivity and flux of the membrane.
  - Non-porous. It presents no detectable pore at the limits of electron microscopy. The membrane is a dense film where permeate diffuses through the membrane material by pressure, gradient. The polymeric material affects the permeability and selectivity of the membrane. The

filtration of solutes occurs from differences in solubility and diffusivity. The disadvantage non-porous membranes presents is low flux, therefore the dense film has to be made extremely thin.

- Anisotropic membranes. The surface layer is supported on a thicker and porous structure.
- Ceramic and metal membranes. Ceramic membranes are used when thermal and chemical stability are needed. Metal membranes are used for hydrogen purification. [6]

3.3 SOLUTE TRANSPORT MECHANISMS THROUGH MEMBRANES

Based on their structure, dense membranes, such as RO membranes, operate on the **solution-diffusion model**, in which solutes dissolve in the membrane material and then diffuse through it due to the concentration gradient. Then the permeants can be separated based on the differences in the solubilities of the solutes in the membrane and the different rates at which different components diffuse through it.

The other model is the **pore-flow model**, associated to porous membranes such as MF or UF membranes, in which solutes are transported by pressure through minuscule pores. Separation occurs because one of the permeants is filtered from some of the pores in the membrane, stopping it from passing through the membrane while other permeants keep progressing.

NF membranes are classified in between porous and dense, thus the model applied may vary depending on the experiment.

The solution-diffusion model operates on the principles of diffusion, the process by which solutes is transported across different parts of the system purely by the presence of a concentration gradient. In an isotropic medium, individually, solutes in the membrane medium are in constant random motion and although its displacement can be calculated the direction is unpredictable. However, if a concentration gradient of solutes is formed in the medium a net transport of matter from the high concentration region to the low concentration region is observed. This concept was first presented in the nineteenth century and the phenomenon was formulated as the equation known as Fick's law of diffusion:

$$J_i = -D_i \frac{dc_i}{dx} \qquad (6)$$

where J_i is the rate of transfer of a certain solute i, D_i the diffusion coefficient, which is a measure of the mobility of individual molecules, and dc_i/dx is the concentration gradient of the i component. The minus sign shows that the direction of diffusion is down the concentration gradient. Diffusion is typically slow, which is why membranes are usually very thin, allowing the creation of large concentration gradients.

Regarding the pore flow model, flows are commonly pressure driven, resulting in a higher flux than simple diffusion based membranes, and its behaviour is expressed

through Darcy's law:

$$J_i = K' c_i \frac{dp}{dx} \quad (7)$$

which takes into account the permeability coefficient, K', which depends on the water viscosity, among other parameters such as temperature, the concentration of component i, c_i, and the pressure gradient in the porous medium, dp/dx.[8]

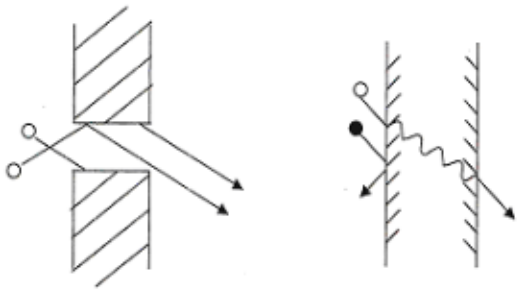

Figure 1 Solution-diffusion model (left) and pore-flow model (right) comparison[8]

The main difference between these two models consists in the relative size and the permanence of the pores. In membranes based in the solution-diffusion model the pores are microscopic spaces between the polymer chains conforming the membrane, caused by thermal motion of its molecules. These free-volume elements appear and disappear at approximately the same rate as the permeants go through the membrane. On the other hand, in membranes based on a pore-flow model, pores are relatively larger and do not fluctuate in position or volume. As a rough estimation, the transition between solution-diffusion and pore-flow pores is in the range of 5-10 Å.[9]

3.4 TRANSPORT PHENOMENA

Regarding the movement the particles experience when in contact with the membrane, three types can be distinguished.

3.4.1 DONNAN EXCLUSION

The Donnan exclusion is a phenomenon that affects the ions, minimising the rejection of all salts and solutes. As expected, this is particularly relevant in ion exchange membranes, where transport of components depends on electric potential gradient. As it can be seen in Figure 2 membrane charge becomes highly relevant as, depending on the charge, cations or anions will have different permeability.

This means that, when under this gradient, cations and anions will move in opposite directions, being able to characterise the membrane in terms of charge transported.[9]

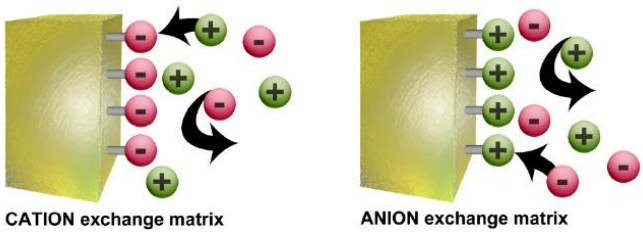

Figure 2 Representation of the Donnan exclusion[10]

However, behaviour of both types of ions does not follow as expected, as the fractions of current carried by the anions and cations are not necessarily the same, generating charge asymmetry. That is caused by the membrane carrying fixed charges, the counter ions of which will show a tendency to be excluded from the membrane. As a result, the concentration of ions of the same charge is reduced, while the concentration of ions of opposite charge is elevated. This makes the membrane selective for ions of the opposite charge.

In brief, the Donnan exclusion expresses the tendency of charged groups tend to exclude ions of the same charge, particularly multivalent ions while being freely permeable to ions of the opposite charge, particularly multivalent ions.[9]

3.4.2 DIELECTRIC EXCLUSION

Dielectric exclusion is caused by the interactions of ions with the bound electric charges induced by ions at interfaces between media of different dielectric constants, in particular, a membrane matrix and a solvent. This causes ions with the same charge to be induced to the media with lower dielectric constant, until they are even, causing repulsion between the two phases, eventually resulting in exclusion of ions.

They take their name from the fact that the interaction with a polarized interface is formally equivalent to the interaction with a fictitious image charge located at the other side of the interface at the same distance from it as the real charge.

The sign and magnitude of the image are determined by the dielectric constants of the media. Thus for instance, a metal attracts ions whereas a dielectric usually repulses them, so we can easily see that the interaction energy is inversely proportional to the distance from the interface.

This transport phenomenon is characterised for its strong dependence on the pore geometry and its variable character as a function of solvent dielectric constant.[11]

3.4.3 CONCENTRATION POLARISATION

Concentration polarisation is the term used to describe the increment of solutes in the solution adjacent to the membrane, causing the concentration of the solution to increase. This factor depends on many variables such as concentration, pressure, diffusion of the components… but effectively results in the reduction of separation capabilities of the membrane.

As a feed stream passes through a membrane an hydrodynamic boundary layer is formed, that poses a mass transfer resistance. If the solutes become retained by the

membrane they start to be concentrated at the membrane surface since transport into the boundary layer is normally higher than diffusion back into the feed bulk.

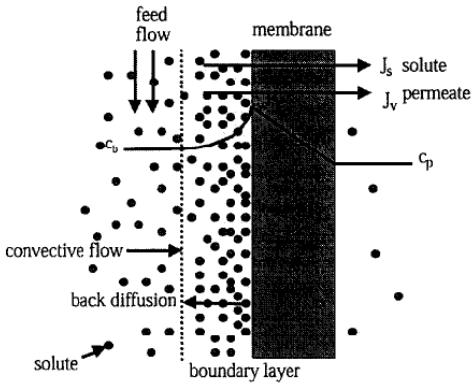

Figure 3 Representation of concentration polarisation[12]

Concentration polarisation is considered to be reversible and can be controlled in the module by different means, such as velocity adjustment or optimising hydraulic conditions of the filtration.[12]

3.5 TYPES OF OPERATION OF MEMBRANES

Regarding the type of operation, membranes can be divided into two groups depending on the direction the flow is moving relative to the membrane.

Knowing the direction of the flow is important in order to avoid fouling, one of the problems of membrane technologies. Fouling refers to the accumulation of solute particles on the surface of the membrane, which happens inherently during the filtration process. As more solute accumulates, it becomes harder for the solution to pass through the membrane, resulting in a loss of performance of the membrane. In order to remove fouling, chemical or physical cleaning methods may be required to restore the original properties of the membrane.

Filtrations can be executed passing the feed tangentially through the membrane, in what is known as cross-flow filtration. In this type of filtration the feed is passed applying a positive pressure relative to the permeate side, allowing a part of the feed to pass through the membrane as permeate, retaining filtered species in the feed side. The main advantage of this method is that it allows the trapped particles on the filter of the surface to be rubbed off, as they are in constant contact with the feed stream, achieving a higher removal rate and extending the lifetime of the membrane. Cross-flow filtration minimises the amount of fouling that occurs on the surface of the membrane.

The other method is known as dead-end (or in-line) filtration where the fluid is forced, by applying pressure, in perpendicular direction in respect to the membrane. This technique has the disadvantage that particles accumulate on the membrane surface, causing the system to require a higher pressure to keep the flow, resulting in the eventual replacement of the membrane. Operating under dead-end filtration causes

more fouling than the cross-flow method.

Although cross-flow filtration uses more complex equipment, industrially it is the preferred method, mainly because the membrane has a higher lifetime.

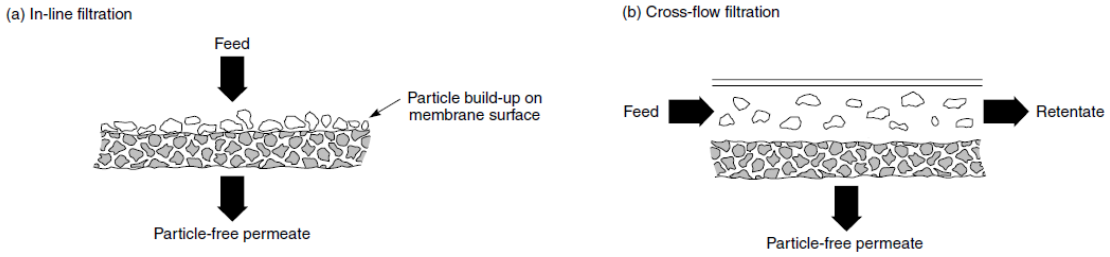

Figure 4 Representation of in-line and cross-flow filtration[11]

3.6 CONFIGURATION OF THE MEMBRANE MODULES

Besides the membrane itself and the system used to pump the water, there is another key element in this type of stations which is the configuration of the membrane module. Effectively, this is where the membrane is contained and supported, and has the purpose of giving the surface of the membrane the desired work conditions.

A first type of module is the plate and frame, which is used by flat sheet membranes, providing a porous support for the permeate. The flow channels are commonly a few millimeters thin, with added spacers occasionally. Feed channel spacers are sheets made of plastic with a grid type pattern, each cell being a few millimeters wide, placed in conjunction to the membrane in order to increase its mass transfer, by improving particle snipping on its surface. Inside the module, membranes are stacked connected to the different flow channels, sometimes providing ondulations on the membrane surface to enhance mass transfer. These modules are used for small to medium size applications since replacing the membranes has to be done sheet by sheet and operating at higher pressures may require plates of considerable size.

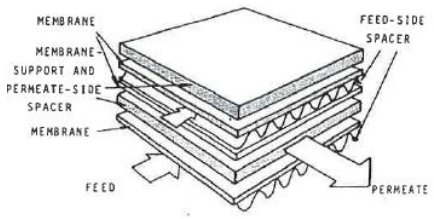

Figure 5 Plate and frame membrane module[6]

There are also spiral-wound modules (SWM), which also use flat sheet membranes, outclassing plate and frame formations in some applications, for example, nanofiltration. Membranes are wound around a central tube, forming sort of ‘blades’ with one side in contact with the permeate. Inside the ‘blades’ spacers are placed to provide additional support to the membrane and prevent it from falling apart due to pressure. Between ‘blades’ spacers are always placed, in contact with the feed, in

order to improve mass transfer. The whole structure is then given an outer casting and flow is passed thorough axially, moving across the blades in a spiral motion toward the center of the tube. It is important to note that due to the spiral motion the fluid follows, a pressure gradient may appear between the center of the tube and the inner wall. It is necessary to minimise pressure drops to obtain optimal conditions.[6]

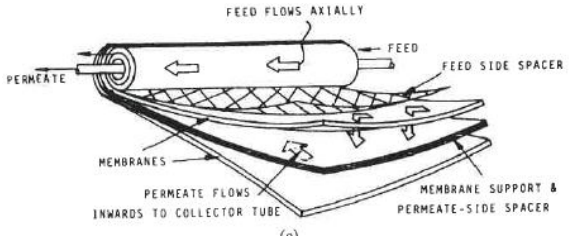

Figure 6 Spiral wound module[6]

4 NANOFILTRATION

Nanofiltration (NF) processes are currently one of the most recent to be introduced in the industry. This method is characterised for being a pressure-driven form of separation, whose characteristics fall between ultrafiltration (UF) and reverse osmosis (RO). At first they were presented as an alternative for water filtration and purification, offering a higher rejection rate than conventional methods, but advances in materials, improvements in the membrane life span and an increasing number of application have made them a reliable process on many different fields, especially in extraction of heavy metals, offering one of the best ratios in terms of economy, environmental benefits and cost.

Regarding AMD treatments, NF offers unique separation opportunities, as, these techniques are characterised for providing low rejection for acids. This means that similar concentrations are achieved on each side of the membrane, minimising the effect on differential osmotic pressure. This property makes NF a highly effective method when dealing with high ionic concentration of strong acid solutions.

4.1 NANOFILTRATION MEMBRANES

In terms of characterisation of the NF membranes, some researchers consider them porous membranes, with a pore size ranges between 0.001 – 0.01 μm. That being said, other reseachers list NF membranes as dense.

Nevertheless, at least, two more factors to be considered that distinguish NF membranes even more from similar methods such as RO and UF. The first of them is the capacity of rejecting multivalent anions, generally achieving complete rejection, as is the case with sulphate and phosphate. The second one is the rejection of sodium chloride (NaCl) which offers a wide range, depending on the system, being able to vary between 70% to 0%.

Listing all these characteristics also implies the fact that separation process in NF membranes is strongly influenced by the charge of the membrane. When measured, it is indeed noticeable that they are usually charged, although rarely at levels as high as UF or RO membranes, implying that the separation not only relies on particle size, but species charge also plays an important part.

Regarding the composition of NF membranes, early designs were made of cellulose acetate (CA), a compound which, by adding additives, could offer a wide range of molecular-weight cutoffs (MWCO), from tight RO up to UF thus including the NF range. It was in the 1970s when the first CA asymmetric (anisotropic) NF membranes were commercially available. The proposed uses were in water-related issues, mainly softening of water purification, as they offered low fouling, easy cleaning and chlorine resistance, although as water treatment processes improved, CA membranes deficiencies became evident.

Another attempt at developing NF membranes to be a common process was made by

utilizing polyelectrolyte complexes, anisotropic membranes made by electrostatic interaction between strongly acidic and basic polyanions and polycations. These membranes never achieved the same range of application as CA membranes, as they had low mechanical strength and variable performance in high-ionic-strength solutions.

Polyamide was also tried as a potential component of membranes. Although it managed to work in the range of NF, it was never able to achieve optimal operation rates. Generally the problem was that not enough flux could be achieved while maintaining good rejection rates, and any potential improvement came at a cost of lower rejection, not offering any real advantage compared to other existing processes.

Lastly, research showed that almost any polymer that forms a homogenous solution in a solvent and a homogenous precipitate could form asymmetric skin structures, thus making them valid for membrane designing. Most of the success was found with sulphonated membranes, such as polysulphone or polybenzoxazindione, but they could either not be cast into selective NF membranes with MWCOs lower than a 1000 or too expensive to be commercialised.

Once the capabilities of NF membranes in a large number of chemical processes were observed, development and improvement was quick, figuring out its flaws and designing membranes more biologically and chemically stable, granting a stable rejection rate and minimising flow loss. In order to satisfy market needs, the membranes had improved solvent, oxidant, pH, biological and mechanical stability, obtained high retention to organic solutes, low rejection of inorganic salts and higher water flux, and selectivities and fluxes that would make them economically viable.

The approach to solve the problems previously stated was to design composite membranes. This method consisted in placing a very thin selective layer over one surface of a finely porous asymmetric UF membrane, usually made of polysulphone or polyethersulphone (PES), resulting in high-salt-rejecting membranes. These composite membranes were produced either by coating the UF membrane with a thin CA film or by carrying out interfacial crosslinking of polyamines with aromatic crosslinkers.

In general, the composite approach is applied to form a thin and hydrophilic selective layer that provides enough water flux, but at the same time crosslinked to the NF extent.

The first successful NF composite membranes were based on the polymerization of an aqueous piperazine film on a polysulphone UF support by hydrophobic aromatic crosslinkers, obtaining NF membranes with high $MgSO_4$ rejection (99%) and low salt retention (<60%).[6]

4.2 INDUSTRIAL APPLICATIONS

As it has already been suggested, high pressure driven NF membranes show more potential in water treatment technologies. NF is capable of generating large quantities of quality water, excelling at removing contaminants from it, decreasing prices for the membranes, lowering energy consumption and showing enhanced membranes

lifetimes compared to similar processes. Industrial uses of NF are focused on environmental applications, mainly treatments for ground water, surface water and wastewater.

4.2.1 GROUNDWATER

Treatment of groundwater by NF is mainly focused on the removal of arsenic (As), a problem that has received increasing attention worldwide. Removal of As by NF membrane was proven successful by integrating a largely fouling-free and highly selective NF membrane, with an upstream pre-oxidation of As (III) to As (V) and a downstream stabilization to treat As rejects. This hybrid system resulted in a continuous removal of >98%.

NF membrane has also been integrated into fertilizer drawn forward osmosis (FDFO) desalination. It was mostly used as a post-treatment, as it managed to reduce nutrient concentrations in final product water, allowing it to be directly applied as a fertiliser without further dilution.

On the same page, pesticide removal has also become quite an important issue, especially as new compounds called pesticide transformation products (PTPs) have been found in groundwater, sometimes emerging to surface sources. Some NF membranes have been successfully used to remove regular pesticides, achieving rates of rejection >90%, but as PTPs are smaller in size, RO has to be used in order to get acceptable rejection.

Finally, NF has also been proven effective as a way of removing fluoride from groundwater, as well as successful removal of radium (Ra), different uranium (U) isotopes and radon (Rn), obtaining a high rejection of 99% without interference of similar ions.

4.2.2 SURFACE WATER

Regarding surface water, the main use of NF has been on water softening, although it has also been proven effective at removing pesticides, disinfection by-products and hormones.

In terms of water softening, NF membranes have become the standard method, as they easily accomplish an around 90% removal rate of magnesium (Mg^{2+}) and calcium (Ca^{2+}) ions, operating at low pressures.

As xenobiotic production and disposition become more common, many surface waters become affected by them. Among these xenobiotics, most popular herbicides are noteworthy due to the toxicity of some of their components such as glyphosate and various surfactants in commercial formulations. NF successfully manage to treat this issue, lowering the concentration of glyphosate in waters containing above five times the lethal dose by >80% (i.e. to non-toxic levels).

Finally, the removal of hormones is crucial when treating drinking water, as they have

been proven to be present in real water sources, such as mestranol or octylphenol, which have endocrine disruption capabilities. Results show above 70% rejection rate of most of the hormones, and this method can be mixed with hormone-degradation techniques such as low pressure indirect photolysis with the addition of hydrogen peroxide.

4.2.3 WASTEWATER

Proper treatment of real wastewater is a difficult issue to tackle that is present in all industrial processes, as wastewater always contains complex matters which are difficult to be separated.

Numerous industrial wastewaters have successfully been treated with NF membranes, such as pharmaceutical or food industry, although the retention and concentration in dyes is one of the largest applications. Various tests have been carried out showing that NF can accomplish complete color removal, and the treated water with good quality can be recycled back into the process, reducing water consumption and improving the overall economy of the process.

4.2.4 DESALINATION

Besides environmental issues, water treatment is also critical to resolve water scarcity. When it comes to water desalination with membrane treatments, two major problems emerge: membrane fouling and high energy consumption. NF membrane has shown potential to overcome these problems as it has applications in pre-treatment of seawater, the treatment of the water and capability to be integrated with other processes to improve performance.

Several studies involving NF as the core of the study have made it common for NF membrane to be integrated in desalination processes, as it offers a lower operating pressure, reducing the costs, and higher production rate than RO. Overall, it has been proven to be not a total substitute, but rather a viable integration to existing processes, as it is most commonly found in conjunction with other methods, such as RO.[13]

4.3 NANOFILTRATION IN ACID MINE DRAINAGE

As it has already been explained, AMD is characterised for having high acidity, high concentration of sulphates, heavy metals and other metals such as REE. All these factors have to be considered when approaching AMD treatment by NF membrane, and, but besides AMD properties, different membranes have different characteristics which also have to be considered to attain optimal results.

4.3.1 ISO-ELECTRIC POINT (IEP)

As it has already been noted, NF membranes show a positive or negative charge, depending on pH and concentration of the solution. The surface becomes charged due to dissociation of the ionizable groups of the polymer that conform the membrane.

One of the first characteristics to be considered is the iso-electric point (IEP) which refers to the solution pH at which the net membrane charge is zero. At pHs higher than the IEP, the membrane becomes charged negatively, and at pHs lower, it is charged

positively.

The scientific literature reports the IEP for different NF membranes. To name a few, Artug and Hapke determined the IEPs of three NF membranes (NF PES 10, NF 2, NF 270) in order to obtain and compare experimental data with similar studies.

Most of commercial membranes have been studied in various conditions, in order to determine their IEP. Some of the results can be found in the table below:

Authors	Membrane	pH range	Solution	IEP
Childress and Elimelech [20]	NF 70	2–9	0.01 M NaCl	4
			0.01 M NaCl + 0.001 M $CaCl_2$	3–3.5
			0.01 M NaCl + 0.001 M Na_2SO_4	4
			0.01 M NaCl + 0.001 M $MgSO_4$	–
	TFCS	2–9	0.01 M NaCl	3
			0.01 M NaCl + 0.001 M $CaCl_2$	3.5
			0.01 M NaCl + 0.001 M Na_2SO_4	3
			0.01 M NaCl + 0.001 M $MgSO_4$	3
Hagmeyer and Gimbel [21]	Desal 5 DK	3–11	0.002 M KCl	4
	NTR-729	3–11	0.002 M KCl	4
Childress and Elimelech [16]	NF 55	3–9	0.01 M NaCl	3.2
			0.01 M NaCl + 2 mg L^{-1} humic acids	no IEP
			0.01 M NaCl + 1 mM surfactants	no IEP
Tanninen *et al.* [22]	NF 270	–	0.001 M KCl	3.3
	Desal 5 DK	–	0.001 M KCl	4.1
	Desal KH	–	0.001 M KCl	4.9
	BTP-NF-1	–	0.001 M KCl	6
	BTP-NF-2	–	0.001 M KCl	5.4
Artug [15]	NF 270	2.5–7	0.001 M NaCl	2.8
			0.001 M $CaCl_2$	3.5
	NF 90	2.5–7	0.001 M NaCl	4.3
			0.001 M $CaCl_2$	4.3
	NF PES 10	2.5–7	0.001 M NaCl	3.4
			0.001 M $CaCl_2$	3.5
	NF 2	2.5–7	0.001 M NaCl	3.2
			0.001 M $CaCl_2$	2.9

Table 3 Different IEP for different membranes and solutions[14]

One of the conclusions provided by studying different NF membranes is that IEP can abruptly vary for each membrane and solution, so study of different species in the solution and diverse operating conditions is key in order to understand the performance of NF membranes and to achieve optimal results. [14]

4.3.2 EQUILIBRIUM SO_4^{2-}/H_2SO_4

Due to the high acidity of AMD, it is common to have high concentrations of sulphates thus recovery of this ion can be important. Depending on the composition and pH of the AMD, the rejection of sulphate by NF can be highly variable.

In the usual range of pH for AMD the following species can be found:

$$H_2SO_4 \rightarrow HSO_4^- + H^+ \quad (8)$$

$$HSO_4^- \leftrightarrow H^+ + SO_4^{2-} \quad (9)$$

The first reaction follows complete dissociation, while in the second one equilibrium can be observed, at a pK_a = 1.92, which means that, at pHs lower than pK_a, hydrogensulphate will be the predominant ion, while at higher pHs, sulphate will present a higher concentration.

Visser et al., 2001 assessed different NF membranes for the removal of sulphuric acid at different concentrations, and, although the removal extent was found different for each membrane, a common tendency was observed for all of them [15].

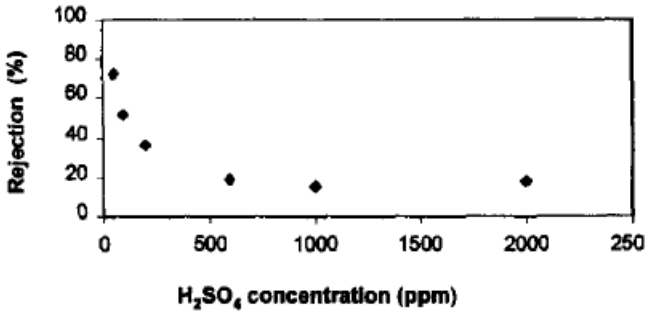

Table 4 Representation of one of the experiments, showing rejection of sulphuric acid vs sulphuric acid concentration[15]

As it can be observed, as sulphuric acid concentration increased, thus decreasing pH, rejection decreased.

The study also determined two expected behaviours:

1. Steeper rejections decrease could be observed as hydrogensulphate concentration became the predominant ion.

2. When the membrane was charged negatively (pH > IEP), higher rejections of anions were observed, while if the charge was positive (pH < IEP) lower rejection of anions was observed.

Finally, it could be generalised that higher concentrations of sulphuric acid meant lower rejection rate, although other factors such as the membrane charge or material can also affect the rejection rate.

4.3.3 Effect of pH

The effects of pH have been also largely investigated by previous studies, as membranes are stable at neutral pH but are forced to work with highly acidic solutions.

In order to study the effect of the pH on the membrane rejection, the simplest case is in presence of a single electrolyte solution. As NF membranes are generally made from polymers, for example, polyamide, it is common for the membranes to not posses dissociable molecules, such as carboxylic or amine groups, exhibiting positive or negative surface charge dependent on pH. For a strong electrolyte, the effect of pH on solute rejection can be explained by electrostatic forces between ions in the solution and the membrane. Generally, salt rejection increases with membrane charge and is

lowest at the IEP of membrane. Rejection of different salts depending on the pH can be seen in Figure 7.

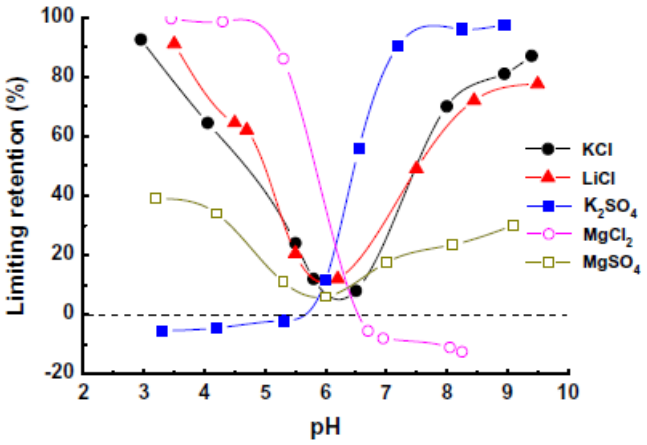

Figure 7 Rejection vs pH of different salts, abrupt changes are experienced at the IEP [16]

As multiple electrolytes are added in the solution, the membranes behaviour becomes more difficult to explain due to the competition amongst different ions. Studies carried by Szoke et al. obtained the following results. [17]

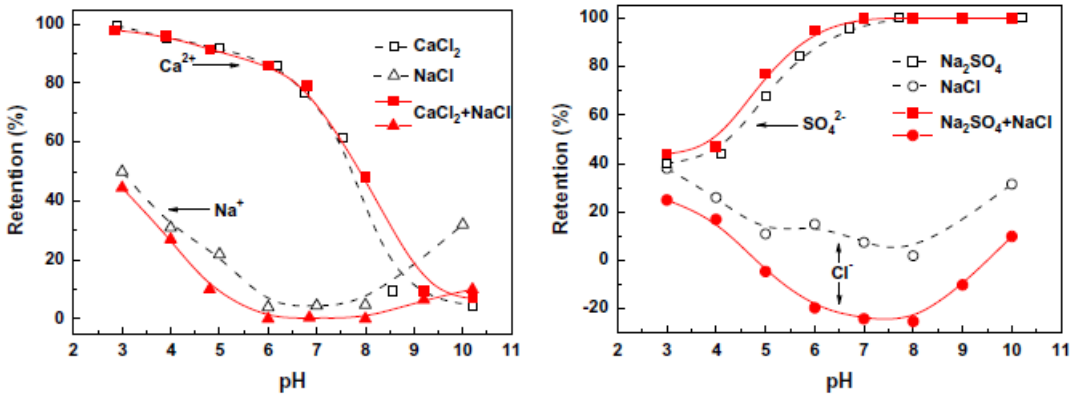

Figure 8 Example of multiple electrolytes rejection curves[16]

One of the thigs that was observed was that, when treating multi-salt solutions, interaction between different ions becomes more relevant, as co-ions competition appears. [16]

5 SOLUTION-DIFFUSION-FILM-MODEL (SDFM)

Modelling is a useful tool for predicting the performance and the scale-up. NF results could be modeled according to the transport mechanisms mentioned before: pore-flow and solution-diffusion model [18-23].

Most of the modelling results of NF have been carried out on the basis of Solution-Diffusion Model. Under the acidity conditions of the experiments, several equilibrium reactions are presented. Only a few attemps to model ion transport flux under equilibrium reactions have been carried out. These calculations require high processing computers due to the high number of variables that must be optimized. [21]

Due to the lack of these equipments, results were modeled according to Solution-Diffusion-Film-Model (SDFM) [24-26], which have been proved to be a good tool for salts, disregarding equilibrium reactions. Model is based on the presence of a high concentrated dominant salt and low concentrated trace ions. Transport takes place by solution-diffusion and electric migration phenomena. Concentration polarization is taken into account, and transport also occurs via convection. Model allows obtaining the membrane permeances to each ion, which is defined as the easiness of the ions to cross the membrane.

Data treatment protocol is carried out as following:

1. From measured trans-membrane flux (Jv) and observable rejection of dominant salt (R_s^{obs}), membrane (P_s) and concentration polatization layer (P_s^{δ}) permeabilities to dominant salt are calculated according to:

$$R_s^{obs} = 1 - {c_s''}/{c_s'} = \frac{{J_v}/{P_s} \cdot e^{-\left({J_v}/{P_s^{\delta}}\right)}}{1 + {J_v}/{P_s} \cdot e^{-\left({J_v}/{P_s^{\delta}}\right)}} \qquad (10)$$

2. Intrinsic rejection and concentration of dominant salt at membrane surface is calculated from measured concentration in the permeate according to:

$$R_s^{int} = 1 - {c_s''}\Big/{c_s^{(m)}} = \frac{{J_v}/{P_s}}{1 + {J_v}/{P_s}} \qquad (11)$$

3. Concentration of trace ion at membrane surface is calculated from measured concentration in the permeate:

$$c_t^{(m)}/c_t' = e^{(Pe_t)} \times \left[1 + R_s^{obs} \cdot e^{(Pe_s)} - 1\right]^{b^{(\delta)}} \times \left\{1 - \left(1 + R_t^{obs}\right) \int_{e^{-(Pe_t)}}^{1} \frac{dy}{\left[1 + R_s^{obs}(y^{-\alpha} - 1)\right]^{b^{(\delta)}}}\right\} \quad (12)$$

Concentration polarization layer thickness is calculated with the diffusion coefficient of ions and with the membrane permeability to dominant salt.

$$\delta = \frac{D_s^{\delta}}{P_s^{\delta}} \quad (13)$$

4. The passage of the trace ion (f_t) could be calculated as a function of the passage of the dominant salt (f_s).

$$f_t = (f_s)^{b^{(\delta)}} + K\left(\frac{f_s - (f_s)^{b^{(\delta)}}}{1 - b^{(\delta)}}\right) \quad (14)$$

5. From previous equation, experimental data could be fitted with b and K.

$$b = \frac{Z_t(D_+ - D_-)}{Z_+D_+ - Z_-D_-}$$

$$K = D_s/D_t$$

6. Membrane permeabilities to ions (of dominant salt or traces) could be calculated as follows:

$$P_{\pm} = \frac{P_s}{1 - \left(Z_{\pm}/Z_t\right) b^{(\delta)}} \quad (15)$$

$$P_t = \frac{P_s}{K} \quad (16)$$

Different variables and parameters are collected in Table 4.

$Pe_{s,t} = J_v \delta / D_{s,t}^{\delta}$ is the Peclet of the dominant salt or trace ion
$D_s^{\delta} = \frac{(Z_+ - Z_-)D_+D_-}{Z_+D_+ - Z_-D_-}$ is the diffusion coefficient in the unstirred layer
$b^{(\delta)} = \frac{Z_t(D_+ - D_-)}{Z_+D_+ - Z_-D_-}$ is the dimensionless diffusion coefficient
$\alpha = D_t^{\delta}/D_s^{\delta}$ is the ratio of the trace ion diffusion respect to dominant salt

$f_{s,t} = \frac{c_{s,t}^{(m)}}{c_{s,t}''} = \frac{1}{1-R_{s,t}}$ is the passage of dominant salt or trace ion

Table 5 Variables and parameters of the diffusion-solution model

6 EXPERIMENTAL METHODOLOGY

The aim of this project is to study different NF membranes to treat AMD. As it has been mentioned before, AMD is an existing problem that has gained special attention in the past years, mainly due to two important reasons. First, they present a serious threat to the environment, so it is necessary to treat them to decrease its environmental impact as much as possible. Secondly, many of the metals dissolved in AMD, mainly heavy metals and REE, have important industrial uses, so there is also an interest in recovering them to be reused.

The experiments were performed in a laboratory-scale plant, using a NF process. The solutions presented the usual composition of AMD, and were treated under different conditions of pH, Al^{3+} concentration and Fe^{3+} concentration, in order to study how the membrane performs and its rejection rate in different circumstances.

6.1 LABORATORY PLANT

All the equipment utilized in order to perform the experiment can be observed in the scheme represented in Figure 9:

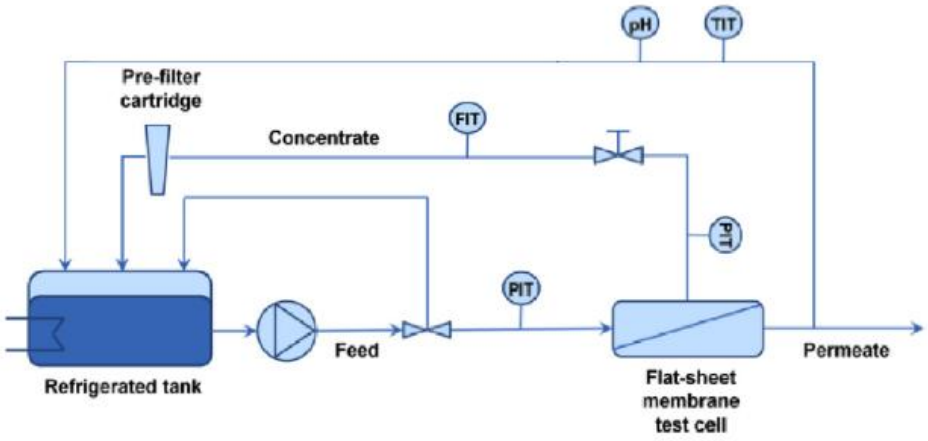

Figure 9 Schematics of the laboratoy plant [27]

As it can be observed, the plant has different elements. The solution treated is stored in the refrigerated tank, which is then forced through the system by the pump. The pump used is a Hydra Cell G-10, and it is connected to the tank by PVC tubes. The tube which connects the pump to the module is made out of steel. Figures 10 and 11 display the pump used and the tubes.

Figure 10 Hydra Cell G-10 Pump

The solution is pumped to the module that contains the membrane, where it is divided in two streams: the permeate, which is the fraction of the feed stream that has been permeated through the membrane, and the concentrate, which is the fraction that has not passed through. Both of these streams are recirculated to the tank, to maintain the initial conditions of the solution that is being treated.

Figure 11 Refrigerated tank and connections to the pump

The tube that reciculates the permeate to the tank allows the stream to be branched to a different path, in order to take samples. Once the sample is collected its pH is analysed off-line via a Crison GLP 21 pH meter and its temperature and conductivity via a Crison GLP 31 EC electrical conductivity meter.

The flux and pressure at which the solution is pumped is adjusted by two valves. One of them is a by-pass valve, installed at the exit of the pump, and the other one is a choke valve, placed at the exit of the module. After the choke valve there is also a pre-filter cartridge which separates any solid impurity that could be into the initial solution. The exit of the filter is directly connected to the tank. Figures 12 and 13 show the filter and the valves.

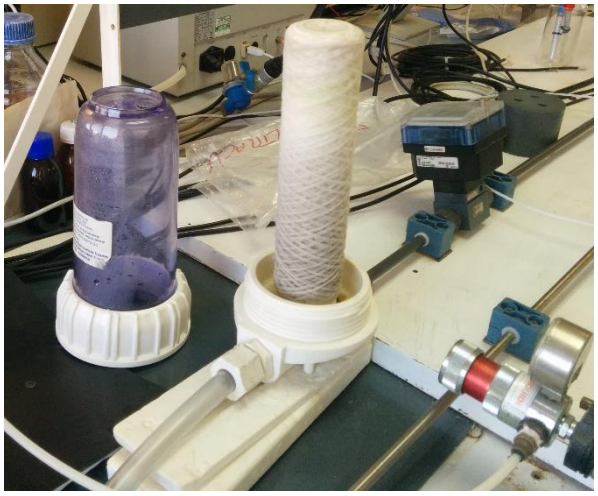

Figure 12 Pre-filter cartridge

Lastly, to measure flux and pressure of the stream the system includes two manometers, one at the entrance and one at the exit of the membrane, and one flow meter placed between the choke valve and the filter. These sensors are connected to a computer which allows the values measure to be stored and processed.

Figure 13 By-pass and choke valves

6.2 EXPERIMENTAL PROCEDURE

After describing the laboratory-scale plant in which experiments where conducted, the procedure carried out for all the experiments is going to be described, from the preparation of the membrane up to the cleansing of the equipment.

- **Membrane**

First of all, the membrane has to be prepared. In order to do so, a piece has to be cut, of the desired size and shape, depending on the module used. In this particular case, a rectangular-shaped piece was cut, with an area of around 140 cm^2. It is also important so submerge the piece in Milli-Q water for at least 24 hours before use, in order to remove any product that may be on the membrane surface for its preservation. After use, it should also be kept submerged in Milli-Q water, to avoid adulteration of the membrane as much as possible.

The membrane used in this experiment was a polyamide DL membrane.

- **Module and plant**

The next step is preparing the NF module in which the membrane will be enclosed. It is composed of a support and a two piece steel box. First of all, the two parts have to be pulled apart, uncovering the space in which the membrane will be placed. Before placing the membrane, two spacers are positioned, one in contact with the entrance of the feed stream and the other with the exit of the permeate. As it was mentioned earlier, they serve the purpose of distributing evenly the solution current inside the module, improving the matter transfer with the membrane thus reducing concentration polarisation and, inherently, fouling.

Two rubber bands are also placed, acting as a joint between the two pieces of the module, allowing proper subjection of both the membrane and the module itself.

The module described, as well as a brief visual scheme of the putting together process, can be seen in figures 14 and 15

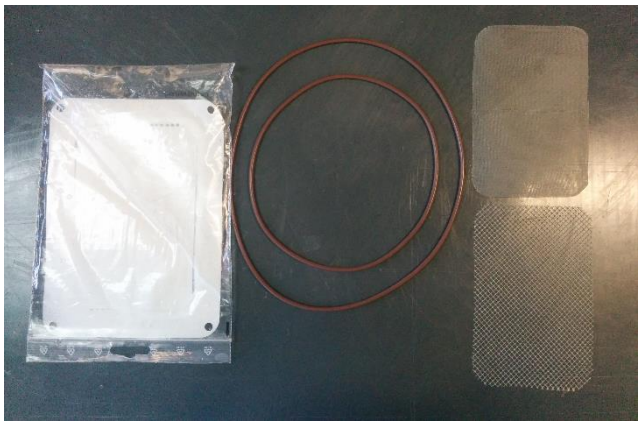

Figure 14 Equipment contained inside the module. NF membrane, rubber bands and spacers, from left to right

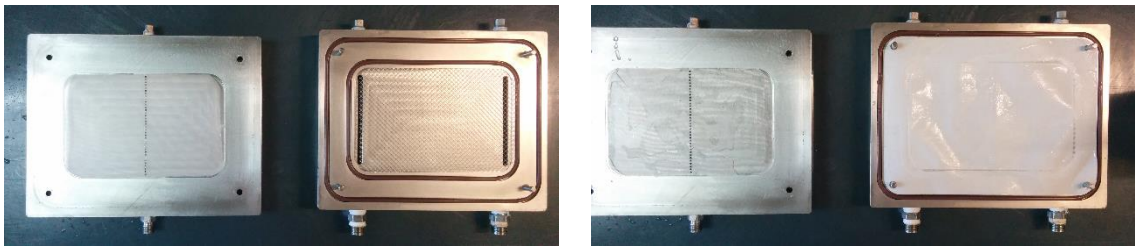

Figure 15 Assembly of all the components. Spacers and rubber bands on the left, inclusion of the membrane on the right

Once the module is ready, it is placed on the support, and connected to the rest of the equipment according to figure 16.

Figure 16 NF module used, indicating connections

Once the module is connected to the rest of the plant, it is pressurised with a manual pump to 40 bar.

Finally, the pre-cartridge filter is installed. It should be kept in proper conditions while it is not being used, in order to prevent microbial growth.

- **Membrane pressurisation with water**

Before carrying out any experiment with the membrane, it is necessary to pressurise it. In order to do so, two different parameters will be adjusted, to the desired operation conditions.

The first of them is the Trans-membrane Pressure (TMP), which is defined by the following equation:

$$TMP = \frac{P_{inlet} - P_{outlet}}{2} - P_{permeate} \quad (17)$$

where:

P_{inlet} is the pressure of the feed stream inlet [bar]
P_{outlet} is the pressure of the feed stream outlet [bar]
$P_{permeate}$ is the pressure of the permeate [bar]

These pressure is regulated with the two valves mentioned beforehand, the by-pass and the choke valve, and, since the pressures measured are relative values, $P_{permeate}$ has a value of 0 [bar], because the permeate outlet is discharged to atmospheric pressure.

The second parameter is cross flow velocity (CFV), which is defined by the following equation:

$$CFV = \frac{Q}{w \cdot t} \quad (18)$$

where:

Q is the flow [m^3/s]
w is the width of the module where flux passes through [m]
t is the height of both spacers and the membrane [m]

Both w and t depend on the module, in this particular case w = 3.75 in and t = 0.034 in.

Equation 11 allows establishing a correlation between CFV and Q, which is represented in figure 17:

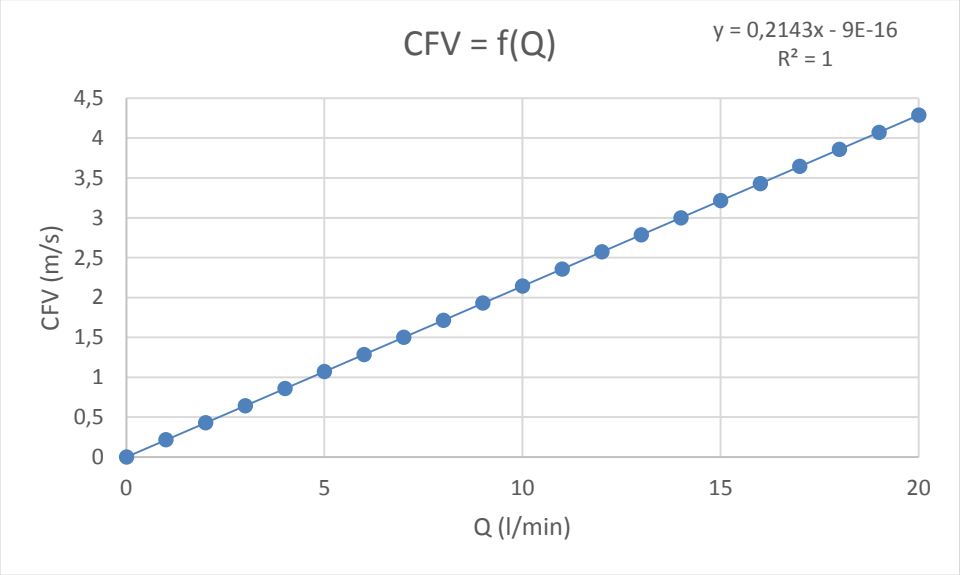

Figure 17 Correlation between Q and CFV

In order to pressurise the membrane, it has to operate at the maximum TMP and CFV values, which correspond to 22 bar and 1 m/s respectively. Since the pump only allows to regulate liquid flow, using the graph from Figure 17, it can be observed that it is needed a flow of about 5 l/min.

Once the operating conditions are met, the sample collection can begin. The procedure consists in collecting samples of around 30 mL every 15 minutes, in exception to the first two which are collected at 25 minutes intervals. This process concludes at 110 minutes. Since water is at 22 bar for a relatively long time, before starting, the water to be used should be cooled down, as temperature will increase thorough the process and the membrane can be damaged.

A total of 8 samples are collected (7 during the experiment and 1 of the starting solution) and, once collected, pH, temperature, conductivity and weight are measured. The vials in which samples will be collected must be weighed beforehand, allowing to calculate the exact volume of liquid collected, using weigh difference and water density.

- **Solution preparation**

The solution studied had a fixed concentration of calcium, copper, zinc, lanthanum, neodynium, samarium, dysprosium, praseodymium and ytterbium. Depending on the solution, either the concentration of iron or aluminum was modified, and also the pH. The change of pH was done by addition of sulfuric acid, which causes an increment of sulphates in the solution. In the cases where iron was added, it was done in the form of ferric chloride, causing chloride ions to be present, in a significant amount, in the solution.

All the elements present to the solution were added in the form of salts, all elements added and their respective salts can be seen in Table 4.

Element	Salt
Aluminum	$Al_2(SO_4)_3 \cdot 18H_2O$
Iron	$FeCl_3 \cdot 6H_2O$
Calcium	$CaSO_4 \cdot 2H_2O$
Copper	$CuSO_4$
Zinc	$ZnSO_4 \cdot 7H_2O$
Lanthanum	$La(SO_4)_3 \cdot 9H_2O$
Neodynium	$NdCl_3 \cdot 6H_2O$
Samarium	$SmCl_3$
Dysprosium	Dy_2O_3
Praseodymium	$Pr(NO_3)_3 \cdot 6H_2O$
Ytterbium	Yb_2O_3

Table 6 Elements, their respective salt, and the concentration at which they were added to the solution

27 L of solution were prepared, and the mass of salt added was calculated using the following equation:

$$m_{salt} = \frac{MM_{salt} \cdot V \cdot C}{p} \quad (19)$$

where:

m_{salt} is the mass of salt to add [g]
MM_{salt} is the molecular mass of the salt [g/mol]
V is the total volume of the solution [L]
C is the concentration desired of the element [M]
p is the purity of the salt

When all the salts are weighed, the solution is ready to be prepared. In order to do so, REE (La, Pr, Nd, Sm, Dy, Yb) have to be prepared by dissolving them in sulfuric acid, since they are not soluble in water. The rest of substances (Al, Cu, Ca, Zn, Fe) can be dissolved in water. Once are the species are dissolved and mixed, water is added until the desired volume of 27 L is reached.

- **Experiment**

Once the solution is ready, the experiment starts with the pressurisation of the membrane. The procedure is the same as the one explained above, when pressurisation with water was explained. The solution is pumped through the plant at 22 bar and 5 l/min. It should also be cooled before starting, to about 14 ºC.

When the membrane is pressurised, the CFV is lowered to 0.7 m/s, which corresponds to a flux of 3,46 l/min, and it is maintained through the rest of the experiment. Pressure is also lowered, starting at a value between 2 and 6 bar, close to the osmotic pressure of the solution. Then the pressure is raised in small intervals, until it reaches between 16 and 18 bar.

In this series of experiments, pressure started at 4.5 bar and ended at 16 bar, taking a total of 8 samples, in addition of one of the solution at the beginning and one at the end.

Samples are taken at each change of pressure, following the procedure also mentioned in the water pressurisation section, vials are weighted before and after collecting the sample, to calculate more precisely the volume of the sample. It should also be noted that it is needed to time the sample-taking process, for every sample individually.

Once the sample is collected, besides the parameters already mentioned, pH, conductivity and temperature are also measured. All the data gathered will be used to calculate values of rejection and permeability of the membrane, which will be detailed in following sections.

The samples collected will be also analysed via ICP, to measure more precisely their composition after the process.

- **Membrane cleaning**

After the experiment is concluded, it is needed to clean the membrane with deionised water, to remove any impurity that may be left on the surface of the membrane.

The cleaning is done in two phases. First, water is pumped to the plant during 30 minutes, at a pressure of 10 bar and flux of 5 l/min. After this, water is changed and it is pumped through the plant for 90 minutes, at a pressure of 22 bar and a flux of 5 l/min, except the last sample, which will be taken at the same flux, but pressure is lowered to 10 bar.

Samples are taken every 15 minutes, following the same procedure that was used during the experiment. Collecting the data is necessary in order to ensure that the permeability of the membrane is the same as the one at the beginning.

If two cleanings are not enough for the membrane to return to its original properties, a third one may be required. Once the cleaning is done, the membrane is ready to be used once again.

6.3 EXPERIMENT DESIGN

A total of 10 experiments were carried out, with the objective to study the rejection of different species varying the pH of the solution and by modifying the quantity of either iron or aluminum dissolved.

The composition of the starting solution can be seen in the table below:

Element	Concentration
Aluminum	12 mM
Calcium	0.6 mM
Copper	0.6 mM
Zinc	0.6 mM
Lanthanum	10 ppm
Neodynium	10 ppm
Samarium	10 ppm
Dysprosium	10 ppm
Praseodymium	10 ppm
Ytterbium	10 ppm

Table 7 Concentration of different elements in the starting solution

These concentrations are the present in all solutions, although, depending on the experiment, other substances may also be present.

Presence of sulphates as ions is expected, as some of the salts are sulphate salts, albeit in some experiments the pH is lowered. So, the concentration of sulphates depends on the volume added to lower the pH to the desired value, ICP analysis of the samples will provide the necessary data.

In a similar note, as it was already mentioned, iron is added in the form of iron(III) chloride, so, experiments that contain iron will also report a significative amount of chloride when analysed via ICP.

The concentration of protons is also taken into consideration, which will be calculated with the pH measure of every sample.

In the table below, all experiments and their conditions are listed.

Experiment	pH	[Fe] ppm	[Al] ppm
1	1.5	---	323.37
2	1	---	323.37
3	1	500	323.37
4	1	1000	323.37
5	1	---	600
6	1	---	900
7	1	---	1200
8	1	---	1500
9	1	1500	323.37

Table 8 Experiment conditions

As it can be seen, the experiments involving the addition of iron could not be carried out consecutively. This was due to a problem with the NF membrane, which had to be replacedWith the new membrane, it was decided to do first all the aluminium experiments. Although the membrane was changed, the model was the same.

The first two experiments correspond to the starting solution, the first one studying the solution at the pH that was achieved just by preparing it, and the second one lowering the pH to 1, which was kept in the rest of experiments.

Experiments 3, 4, 9 studied the presence of iron in the solution, from 500 to 1500 ppm. Since the addition was done on top of the starting solution, 12 mM of aluminium are also present in all cases.

Finally, experiments from 5 to 8 studied how aluminium affected. Starting at 323 ppm (12 mM), at experiment 2, to 1500 ppm.

When comparing the results, the samples will be commented in terms of composition and not number of experiment.

6.4 SAMPLE ANALYSIS

6.4.1 ION CHROMATOGRAPHY

Ion chromatography is based on the transfer of one solute from one mobile phase to other stationary. Samples are injected (mobile phase) to the flow of a eluent and in flows through an ion exchange column (stationary phase). Ion are separated from eluent and are retained in the column. Retention time will be a function of affinity between ion and column.

Ion analysis were performed on a Dionex ICS-1100 column for anion analysis. The IONPAC®AS23 anion—exchange column uses a mixture of 0.0045 M Na_2CO_3 and 0.0008 M $NaHCO_3$. Standards were prepared in a fitting concentration range, so the concentration of the samples would be in the center of the curve.

Retention capacity of the columns is limited to 300 ppm, so samples were diluted before the injection in the column.

6.4.2 INDUCED COUPLED PLASMA (ICP)

ICP is an analytical technique used for elemental determinations, specially powerful in the determination of trace elements in a large amount of samples.

This procedure is classified under atomic emission spectroscopy, where atoms are pushed to an excited state, by applying heat, resulting in the emission of radiation. Once that state is achieved, each element is determined based on the wavelength at which it is emitting, since it is different for all of them.

This method in particular, relies on achieving high temperatures by the ionisation of a gas, argon specifically. The ionisation is achieved by applying a spark to the gas, causing the electrons to be stripped off and forming ions, which will be caught in the magentic field already present, induced by a coil, causing them to collide with other

argon ions, resulting in an argon plasma. The resistance presented by the electrons and ions to the movement caused by the magnetic field is what causes the heating.

The sample is then introduced into the ICP plasma as an aerosol, and they are first converted into gaseous atoms and then ionised towards the end of the plasma.

Finally, by analysing wavelengths and the intensity at which the radiation was produced, results are obtained. [28]

Samples were analysed by an external laboratory, the Institut de Diagnosi Ambiental i Estudis d'Aigüa (IDAEA) of the Consejo Superior de Investigaciones Científicas (CSIC).

7 ANALYSIS OF THE RESULTS

In this chapter it will be explained how the results were obtained, as well as discussion and comparison with different experiments carried out in similar conditions.

7.1 PARAMETERS STUDIED

First, it will be explained how the parametres were calculated.

One of the first that was calculated is the trans-membrane flux (J_v), following the next equation:

$$J_v = \frac{Q_p}{S_m} = \frac{V_p}{t_p S_m} = \frac{\frac{m_p}{\rho}}{t_p S_m} \quad (20)$$

where:

Q_p is the permeate flux [m^3/s]
S_m is the surface of the membrane in contact with the flux [m^2]
V_p is the volume of permeate gathered in the sample [m^3]
t_p is the time that was needed to take the sample [s]
m_p is the total mass of permeate in the sample [kg]
ρ is the density [kg/m^3]

J_v gives expresses the flux generated associated to time and surface [m^3/m^2 s].

This is then used to obtain the membrane permeability (K_w), which expresses how fluent the dissolution passes through the membrane [m^3/m^2 s bar].

$$K_w = \frac{J_v}{TMP} \quad (21)$$

where J_w was just defined and TMP refers to the trans-membrane pressure, also defined earlier. When discussing results, data will be modelled to express permeability of a single element opposed to the whole solution, as results will be more representative.

Also, for each sample, the rejection (R) the membrane offered is also calculated.

$$R = \frac{C_f - C_p}{C_f} \quad (22)$$

where:

C_f is the conductivity of the feed [mS/cm]
C_p is the conductivity of the permeate [mS/cm]

As two sample of the feed were taken, one at the beginning of the experiment and one at the end, C_f will be calculated as the average between both values, in order to obtain a more accurate value.

7.2 REJECTION

The solutions will be compared by associating rejection (R) to trans-membrane flux (J_v).

First, the solutions without any iron nor aluminium, besides the starting 12 mM, will be compared. This results intend to show the effect lowering pH has on the membrane in terms of rejection.

Then, the rest of the solutions will be compared, grouping the ones where iron was added and the ones where aluminium was added. As pH remains the same across all experiments, the aim is studying the impact of increasing the concentration of these metals.

7.2.1 EFFECT OF PH

As mentioned, in the following graphs (Figures 18 and 19), the results obtained are represented.

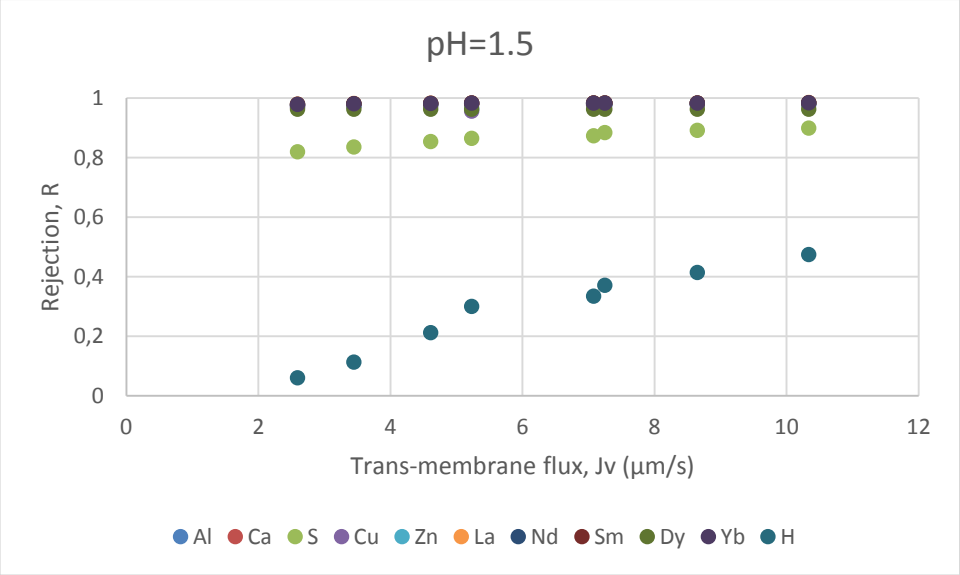

Figure 18 Rejection of the starting solution at pH=1.5

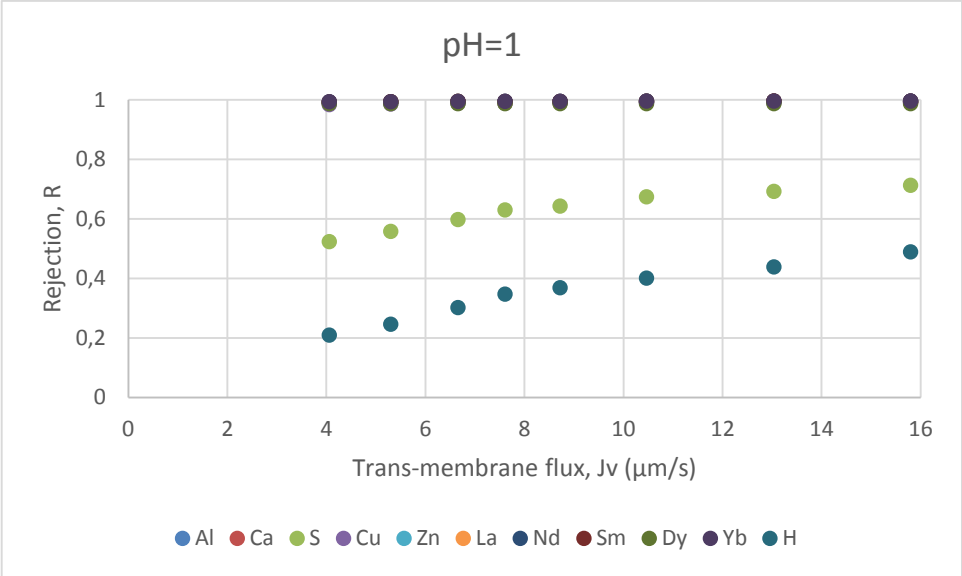

Figure 19 Rejection of the starting solution at pH=1

As it can be easily seen, the results show that the membrane presented significant rejection values for most of the species. As expected, the membrane's rejection increases as the flux increments. Looking at the data in more detail, excluding sulphur and hydrogen, while operating at pH=1.5 the membrane offered an average rejection of around 98%, while at pH=1 it was above 99%. It was also expected that the membrane would offer better rejection to cations at lower pH values, due to the iso-electric point (IEP).

The membrane used has an IEP=3, and, while the experiments were conducted at a pH lower than the membrane's IEP in both cases, the further the pH value is in relation to the IEP, the higher the rejection is. In this situation, the membrane becomes charged positively, which means that a higher rejection of positively charged ions will occur, while negative charged ions will easily pass through more easily.

This phenomenon will also explain the different results that one of the elements shows. Sulphate shows lower rejection compared to the rest of the elements due to being present in two different ions, sulphate (SO_4^{2-}) and hydrogensulphate (HSO_4^-). Where each anion is more prevalent can be seen in Figure 20 which depicts the fraction diagram.

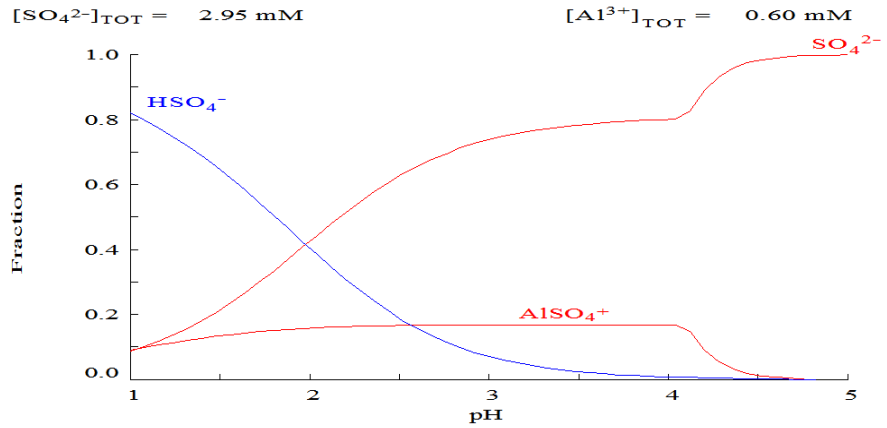

Figure 20 Fraction diagram for sulphate

This diagram is based on the conditions of the first experiment, although simplified, as only aluminium and sulphate were added, since other elements do not affect the outcome due to its low concentration.

As it can be seen, both at pH=1 and pH=1.5 hydrogensulphate is the predominant ion, opposed to sulphate. Rejection shows a correlation between the charge of the ion, as, the higher the negative charge, the higher the expected rejection is, so, as the solution contains mostly hydrogensulphate, the membrane does not reject it as effectively as sulphate. This is in agreement with dielectric exclusion phenomena.

This is also relevant when comparing the sulphur rejection at both pH, as rejection at pH=1 is significantly lower that at a higher pH (decrease of 20 %). Following the same reasoning, the fraction diagram shows that at lower pH the fraction of hydrogensulphate is higher, resulting in more sulphur passing through the membrane.

Finally, hydrogen rejection curve also stands out from the rest of elements, showing significant lower rejection. This could be attributed to electroneutrality principle. The low passage of divalent and trivalent cations makes hydrogen more permeable. This is also in agreement with dielectric exclusion phenomena. Other reason could be the displacement of hydrogensulphate equilibrium towards hygrogen and sulphate formation.

7.2.2 EXPERIMENT AT PH=1 AND 500 PPM OF IRON

In this case, the conditions of the solution are the same, varying the concentration of iron, which is 500 ppm.

Figure 21 shows membrane rejection versus trans-membrane flux.

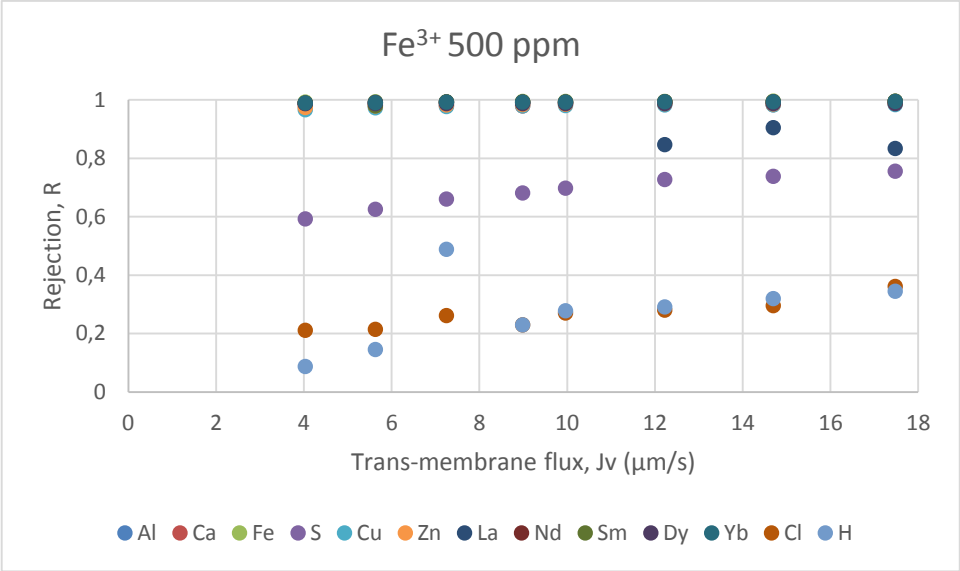

Figure 21 Rejection of the soluttion with 500 ppm of iron

As it can be observed, similarly to the cases considered in the previous section, most of the elements show high rejection rate, with a few exceptions.

For trans-membrane fluxes above 12 µm/s, the rejection of lanthanum significantly descends, showing values of rejection >99% in the first samples while in the last ones values are <90%. This is most likely result of experimental error, as no other experiment nor element shows, or should show, this behaviour.

Sulphur and hydrogen curves present similar results to the experiments from the previous section, as their rejection is lower than the rest of elements, although sulfur rejection is slightly higher than in the former one. This increment is due to the formation of complexes of different sulphur cations with iron, which can be seen in Figure 22. Reasoning for the lower rejection is the same as the one mentioned in the first two experiments.

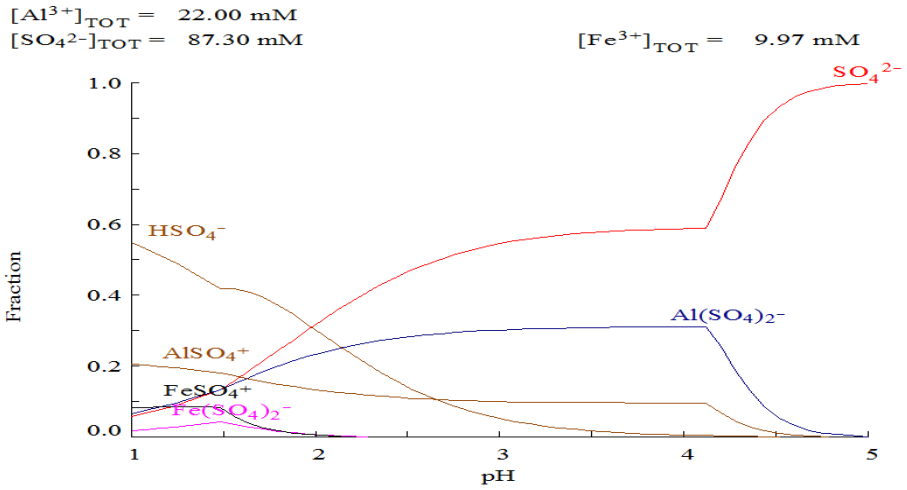

Figure 22 Fraction diagram for sulphur at pH=1 and 500 ppm of iron

The curve represented for chlorine, which was not present in the other solutions commented so far, shows similar behaviour as the hydrogensulphate and sulphate. It is a negatively monocharged ion, while the membrane is charged positively, so rejection is lower than cations.

Iron, being the main difference with the previous section, showed rejection values >99% for all trans-membrane fluxes, averaging 99.4%. For the rest of metals, rejection average is 98.2%, being >99% at higher trans-membrane flux.

Membrane permeability was $9.84 \cdot 10^{-7}$ m^3/m^2 s bar.

7.2.3 EXPERIMENT AT PH=1 AND 1000 PPM OF IRON

In the following experiment, the conditions are kept the same as earlier, increasing the concentration of iron in the solution. Results are shown in Figure 23.

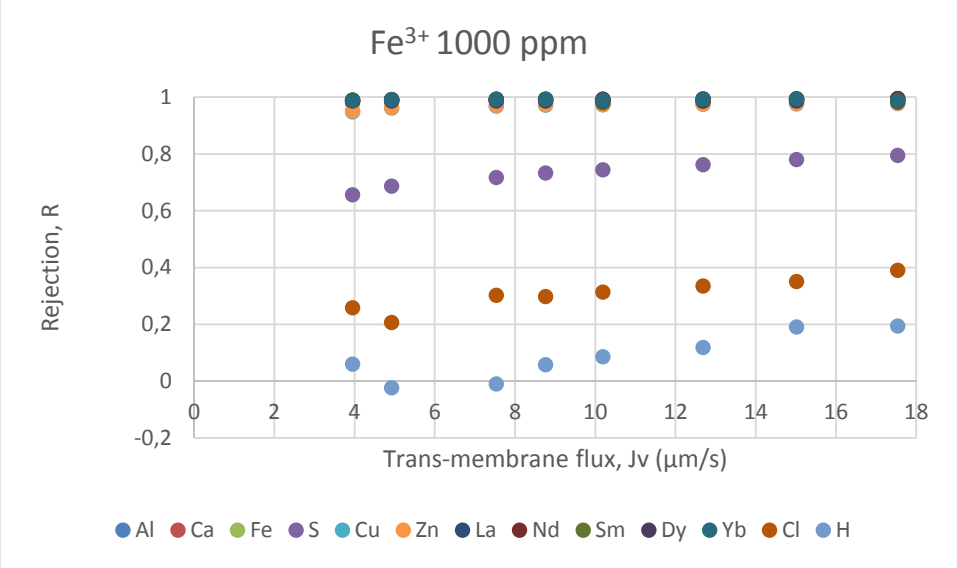

Figure 23 Rejection of the soluttion with 1000 ppm of iron

In this case, the curves show the same tendency as the experiments above.

Rejection for all REE is >99%, showing increasing tendency as trans-membrane flux increments.

The rest of metals, with the exception of zinc, show similar values as the previous experiment, achieving values between 98% and 99% at all times, although higher when more pressure is applied. Zinc starts at a lower rate, around 95%, however 98% rejection is reached at 12.68 µm/s.

Sulphur rejection remains lower than the rest, however, as more iron is added, its rejection keeps increasing, for the same reason as stated above.

Chloride remains approximately in the same range as before, and, even if some values are higher, changes are not significant enough.

Finally, hydrogen shows negative values, at lower trans-membrane fluxes, however, it is also due to the principle of electroneutrality.

7.2.4 EXPERIMENT AT PH=1 AND 1500 PPM OF IRON

Same conditions as before, with a higher concentration of iron. Results are shown in Figure 24.

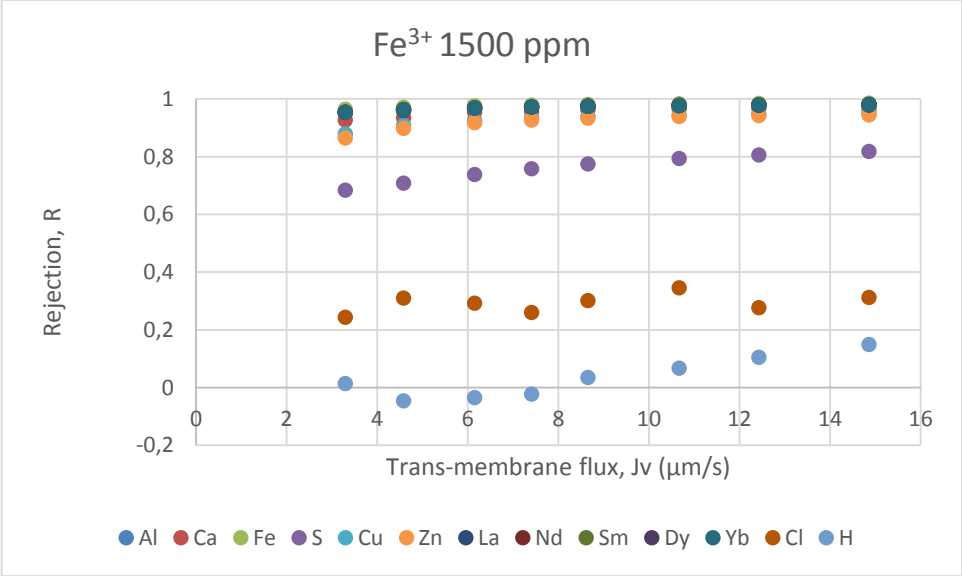

Figure 24 Rejection of the soluttion with 1500 ppm of iron

In this case, all metals and REE start at a significantly lower rejection, increasing as the pressure does. Starting value is around 95%, in exception of zinc, which starts at 87%, but at the end it increases to 98%, also excepting zinc, which increases to only 95%.

This difference may be influenced by the change of membrane. Although it was the same model, this was the first iron experiment carried out after changing it, and at this point all four experiments where aluminium was added were already done, so it is possible that the membrane was more worn-out.

Sulphur rejection is higher than previous experiments, as explained before.

Chloride and hydrogens show no significant differences to previous experiments.

At the end of the experiments including iron, membrane permeability was $8.41 \cdot 10^{-7}$ m^3/m^2 s bar. As iron was being added, permeability lowered.

7.2.5 EXPERIMENT AT PH=1 AND 600 PMM OF ALUMINIUM

The following experiment was conducted at the same conditions and composition of the starting solution, without any iron dissolved and by adding aluminum up to 600 ppm. Results are shown in Figure 25.

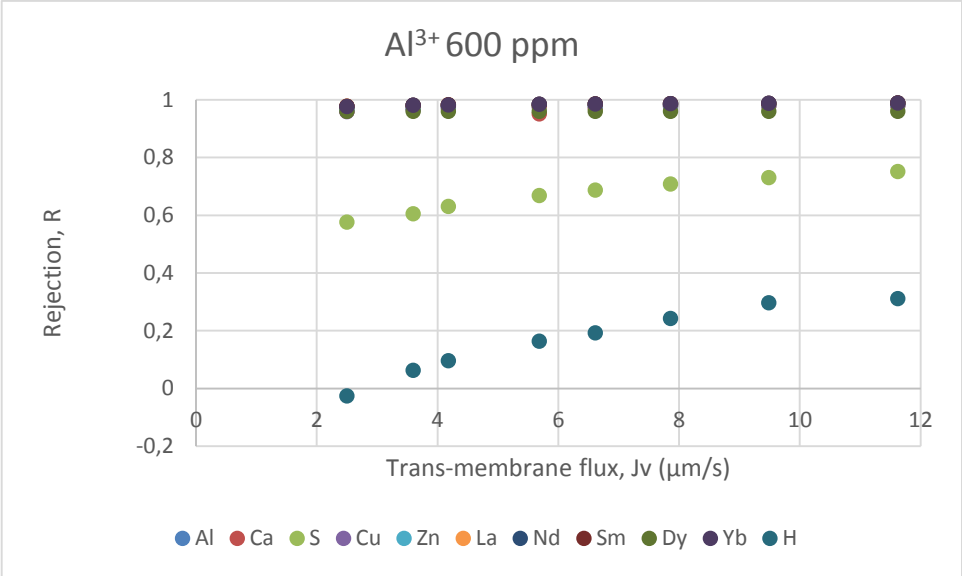

Figure 25 Rejection of the soluttion with 600 ppm of aluminium

When adding aluminium, rejection shows similar values. For all metals and REE, at lower flow starts at around 97%, increasing up to >98%. Compared to the experiment at pH=1 (without any added iron or aluminium, besides the starting 12 mM), rejection, on average, is about 1% lower.

Sulphur mostly shows the same tendency as the solution at pH=1, ranging between 60% and 80%. If results are compared with experiment at pH=1, sulphate rejection barely varies, although it slightly increases, as more sulphate bonds with aluminium forming complexes.

Hydrogen stay at the bottom of the graph, showing lower rejection at higher fluxes than the solution at pH=1 with 12 mM of aluminium.

The membrane permeability is $6.24 \cdot 10^{-7}$ m^3/m^2 s bar.

7.2.6 Experiment at pH=1 and 900 ppm of aluminium

Under the same conditions of the last experiment and increasing the amount of aluminium dissolved, the results are shown in Figure 26.

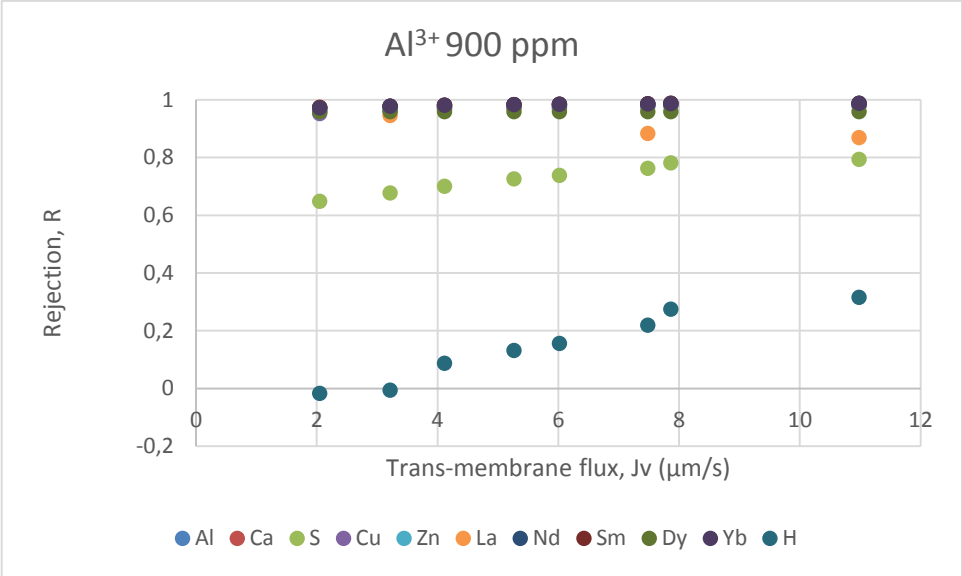

Figure 26 Rejection of the soluttion with 900 ppm of aluminium

In this instance, all metals and REE, with the exception of lanthanum, show an average rejection of 98%. In the case of lanthanum, there are two cases where rejection is lower, around 87%. Although the reduction of rejection at later stages of the experiment could indicate membrane fouling, it is more likely that they are result of experimental error, as the membrane had only been used in one experiment and, at 7.8 µm/s, rejection of lanthanum is >98% and does not follow the lowering tendency. Also no other element shows signs of decreasing rejection.

Sulphur rejection is slightly higher that the previous experiment since, as aluminium concentration rises, more sulphur is present as $Al(SO_4)^+$, which is easier to reject for the membrane.

Hydrogen rejection stays in the same range.

7.2.7 EXPERIMENT AT PH=1 AND 1200 PPM OF ALUMINIUM

At the same pH, increasing the concentration of aluminium to 1200 ppm, we obtain the results shown in Figure 27.

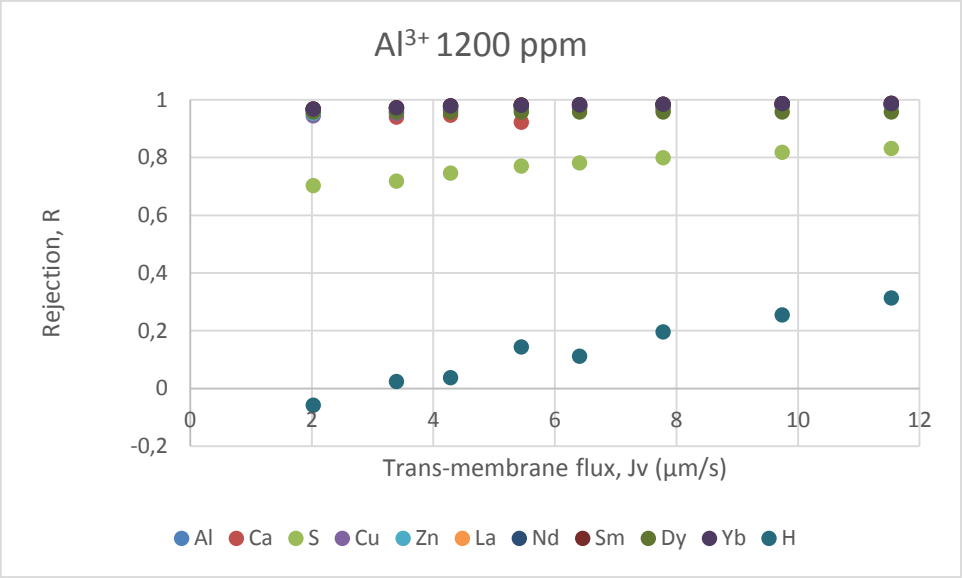

Figure 27 Rejection of the soluttion with 900 ppm of aluminium

The tendency is the same as observed in previous experiments for all metals, although rejection achieved is slightly lower, averaging 97%. Differences are mostly at higher pressures, as starting rejection is very similar compared to the last experiment, excepting calcium, which starts at a lower value but at around 6 µm/s achieves >98%

As expected, sulphur rejection increases overall, as it shows higher values at lower and higher trans-membrane flux, attaining an 83%.

Hydrogens show no significant change.

7.2.8 Experiment at pH=1 and 1500 ppm of aluminium

The results upon adding aluminium until 1500 ppm are shown in Figure 28.

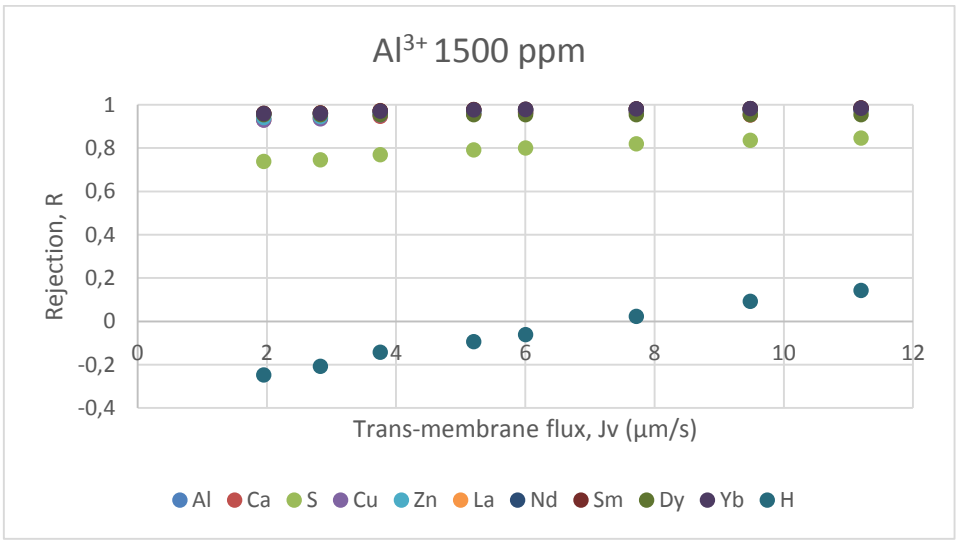

Figure 28 Rejection of the soluttion with 1500 ppm of aluminium

In this experiment, all metals start at a lower value, between 93% and 95%. As pressure augments, rejection also does, getting at 98% at higher trans-membrane flux.

Sulphur shows the most significant change, obtaining a maximum rejection of 85%.

Hydrogens start at -25% and increase to a maximum of 14%, far lower than other experiments.

Membrane permeability is $5.75 \cdot 10^{-7}$ m^3/m^2 s bar, lower than the value at the beginning.

7.3 COMPARISON WITH OTHER MEMBRANES

The values of rejection obtained will be compared with a similar project carried out with the membranes NF-270 (based on semi-aromatic polypiperazine-amide active layer) and Hydracore70pHT (based on poly-ethersulphone sulphonated active layer), in which solutions treated had the same conditions as this study.

Graphs compared will be rejection as a function of trans-membrane flux for lanthanum, sulphur and hydrogent at pH=1. Figures 29 to 31 show the results obtained in the previous study.[29]

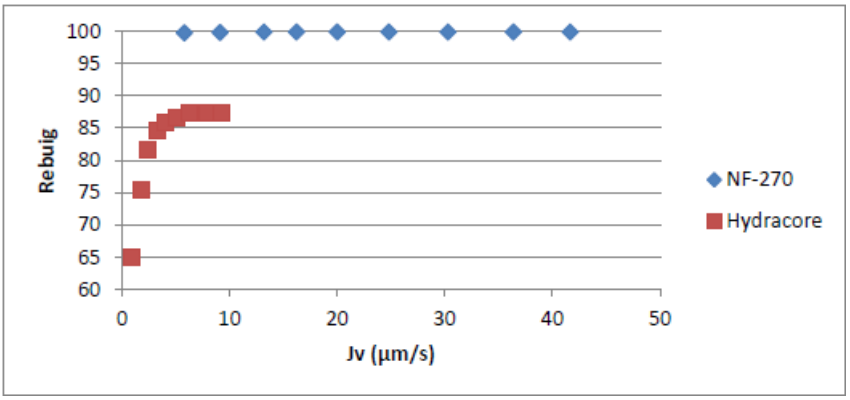

Figure 29 Rejection of lanthanum at pH=1 for membranes NF-270 nd Hydracore 70pHT [29]

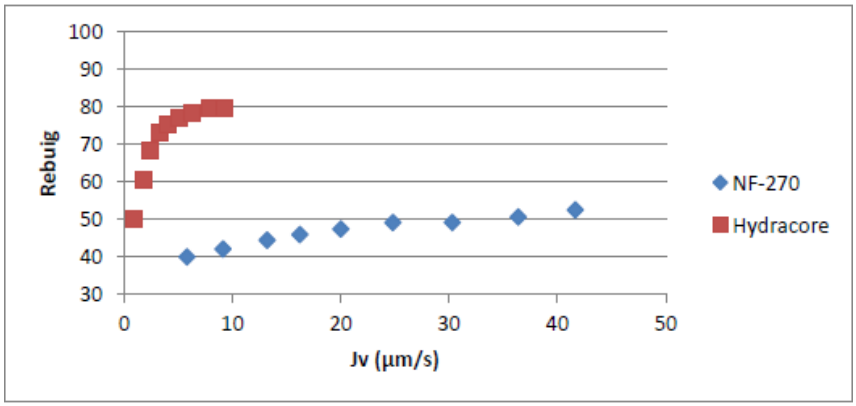

Figure 30 Rejection of sulphur at pH=1 for membranes NF-270 nd Hydracore 70pHT [29]

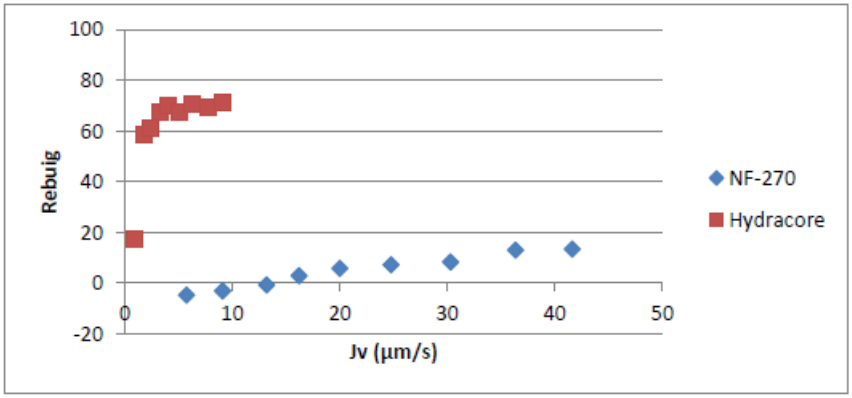

Figure 31 Rejection of hydrogen at pH=1 for membranes NF-270 nd Hydracore 70pHT [29]

Figure 32 shows the results obtained in this study.

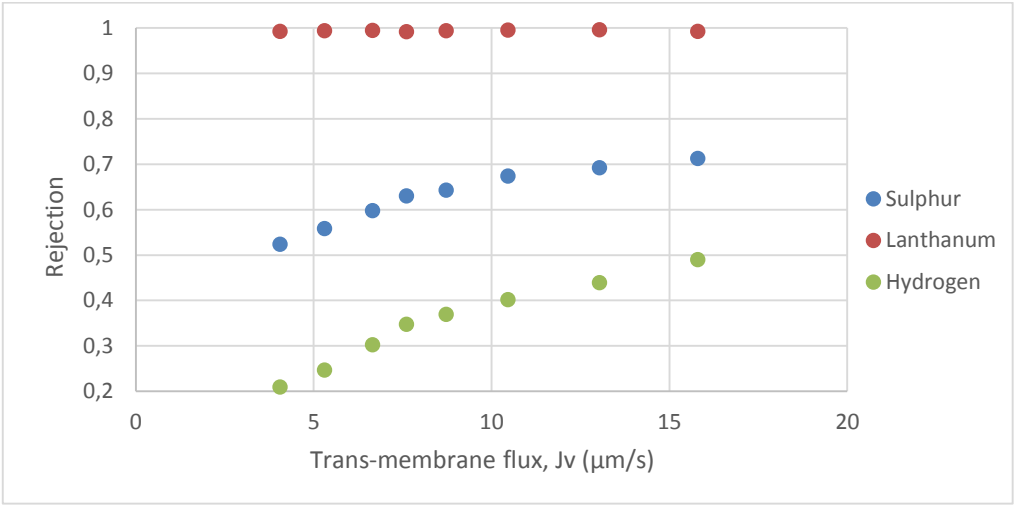

Figure 32 Rejection for lanthanum, sulphur and hydrogen at pH=1

The first thing that can be seen is that the membrane used in this experiment had trans-membrane flux values higher to the Hydracore membrane, although similar, while the NF-270 model worked at over 40 µm/s. That means that the NF-270 model requires less energy to reach the same flux as both the other membranes.

Regarding the rejection, lanthanum was rejected at >99%, which appears to be very similar to the values obtained with the NF-270 membrane, while the Hydracore rejection rate was below 90%.

Hydracore showed the highest sulphur rejection rate, peaking at around 80%, while in this study peak value was 71.3%. NF-270 showed the worse values, peaking slightly above 50%.

Finally, Hydracore had also the best rejection to hydrogen, peaking at around 70%. NF-270 model showed the lowest one, being <20% at all time, while the one studied in this project starts at around the same value as the Hydracore, but at its maximum it only achieves 49%.

Differences on rejections and trans-membrane fluxes could be attributed to the composition of the active side of the membrane. NF-270 and Desal DL (both polyamides) presented similar rejections, meanwhile Hydracore showed major differences if compared.

7.4 MEMBRANE PERMEABILITY TO IONS

In this section, the permeability to ions will be evaluated, but in order to do so, some considerations need to be determined first.

To understand NF membranes behaviour in multiple-electrolyte solutions, it is required to know membrane transport properties with respect to single ions. This is due to the fact that transport properties caused by cations and anions can be modified by spontaneously arising electric fields. When using trace ions, these electric fields have more effect than the rejection of single salts, however, if trace ion concentrations are low enough, the membrane properties are unaffected.

Since trace ion concentrations are low respect to the dominant salt, permeability will be modelled choosing a dominant salt, either $Al_2(SO_4)_3$ or H_2SO_4, for each experiment, based on which ion shows higher concentration in the feed. Then, permeability is calculated assuming only a single trace ion is also in the solution, for every trace ion. [30]

This will be determined for eight of the experiments, corresponding to the four that iron was added and the four where aluminium was added, in order to see how permeability varies as one of those metals is added. It was found that the value of membrane permeability of ions is a function of concentration, and follows the next relationship [25]:

$$P_i = a_1 \cdot C_i^{a_2} + a_3 \qquad (23)$$

Where a_1, a_2 and a_3 are parameters that were calculated.

7.4.1 EXPERIMENTS WHERE PH WAS LOWERED

First, the two experiments where pH was lowered will be studied. Figure 33 and Figure 34 show the results obtained with the model for the experiments at pH = 1.5 and pH = 1, respectively. The points represent the experimental data and lines the results obtained with SDFM model. Good agreement was obtained between model and experimental data.

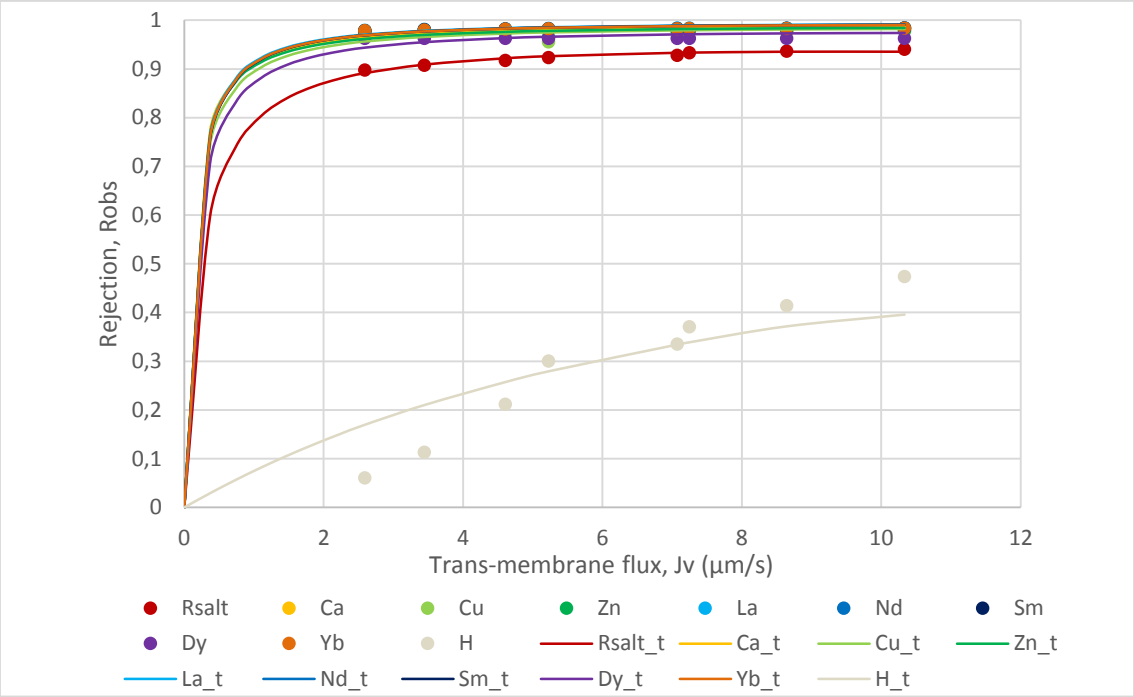

Figure 33 Results obtained with the model for the solution at pH=1.5

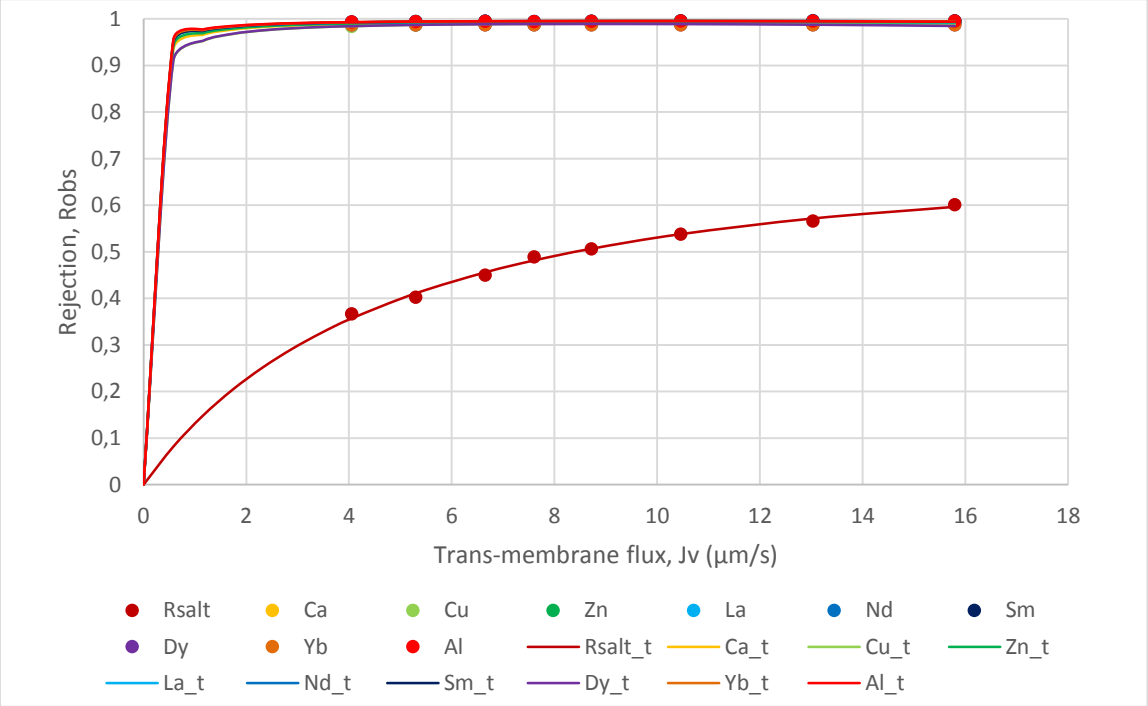

Figure 34 Results obtained with the model for the solution at pH=1

And below, a table with dominant salts for each experiment and permeability for single ions. Results could not be compared with published data because at our concern, there are no works at the acidity, membrane and elements at which experiments were carried out.

Experiment conditions	Dominant Salt	Permeability (µm/s)	
pH=1.5	$Al_2(SO_4)_3$	Ca^{2+}: 0.25 Cu^{2+}: 0.32 Zn^{2+}: 0.27 La^{3+}: 1.10 Nd^{3+}: 1.32	Sm^{3+}: 1.32 Dy^{3+}: 0.46 Yb^{3+}: 1.21 H^{+}: 3.59 Al^{3+}: 0.15 SO_4^{2-}: 0.40
pH=1	H_2SO_4	Al^{3+}: 0.03 Ca^{2+}: 0.04 Cu^{2+}: 0.06 Zn^{2+}: 0.04 La^{3+}: 0.03 Nd^{3+}: 0.03	Sm^{3+}: 0.03 Dy^{3+}: 0.06 Yb^{3+}: 0.03 H^{+}: 10.66 SO_4^{2-}: 0.95

Table 9 Permeability for single ions and dominant salts

7.4.2 EXPERIMENTS WITH IRON

Fitting of experimental results when iron was added is shown in Figures 35 to 37. Points represent the experimental data and lines the results obtained with SDFM model.

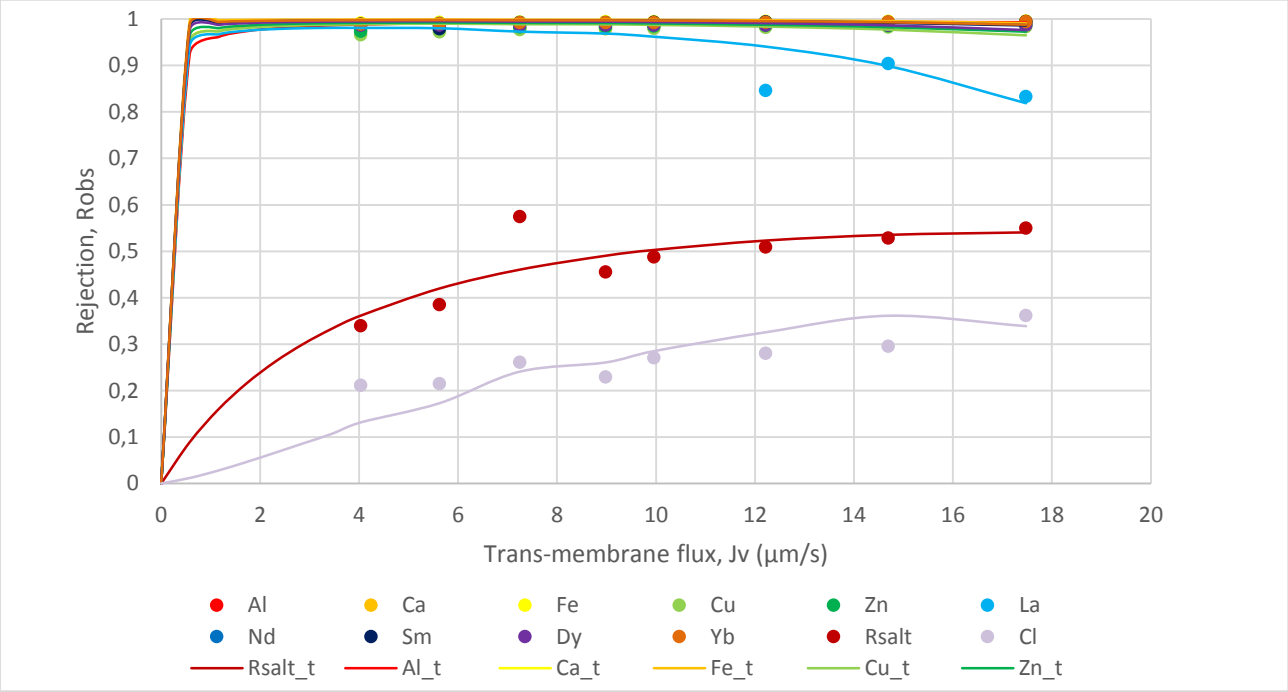

Figure 35 Results obtained with the model for the solution pH=1 and 500 ppm of iron

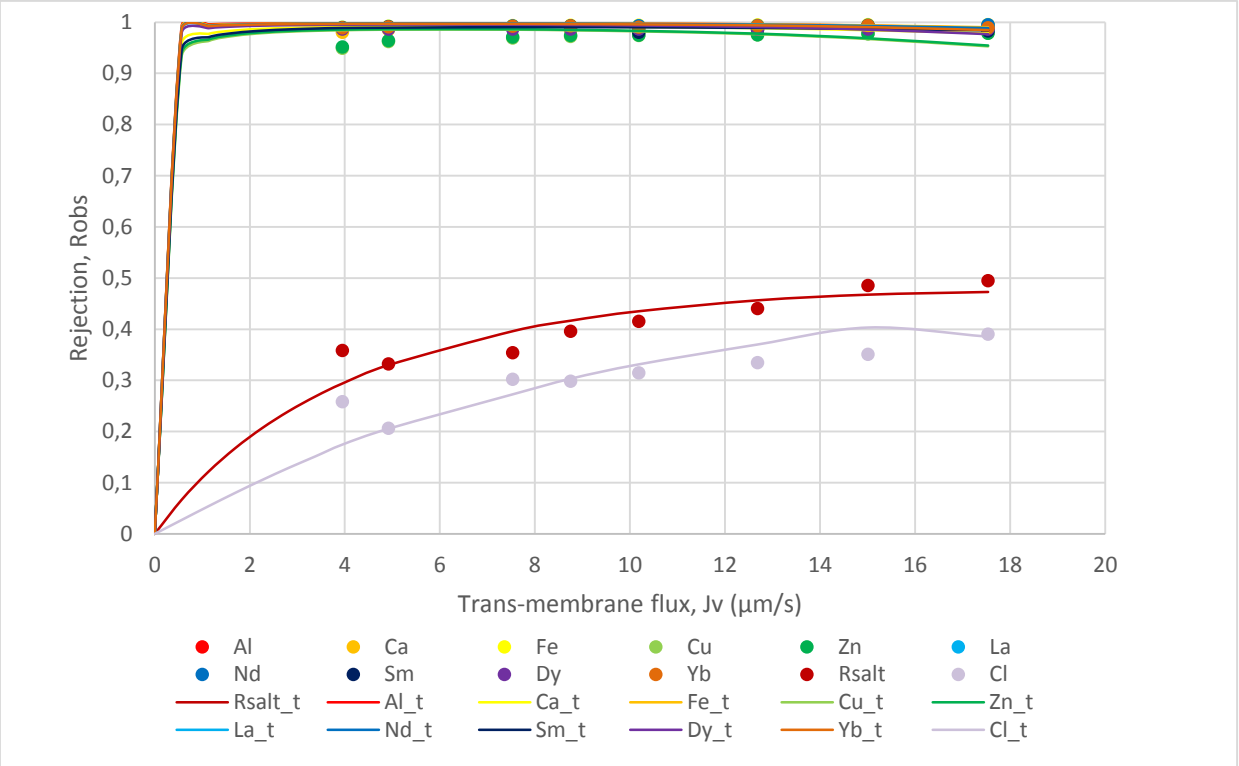

Figure 36 Results obtained with the model for the solution at pH=1 and 1000 ppm of iron

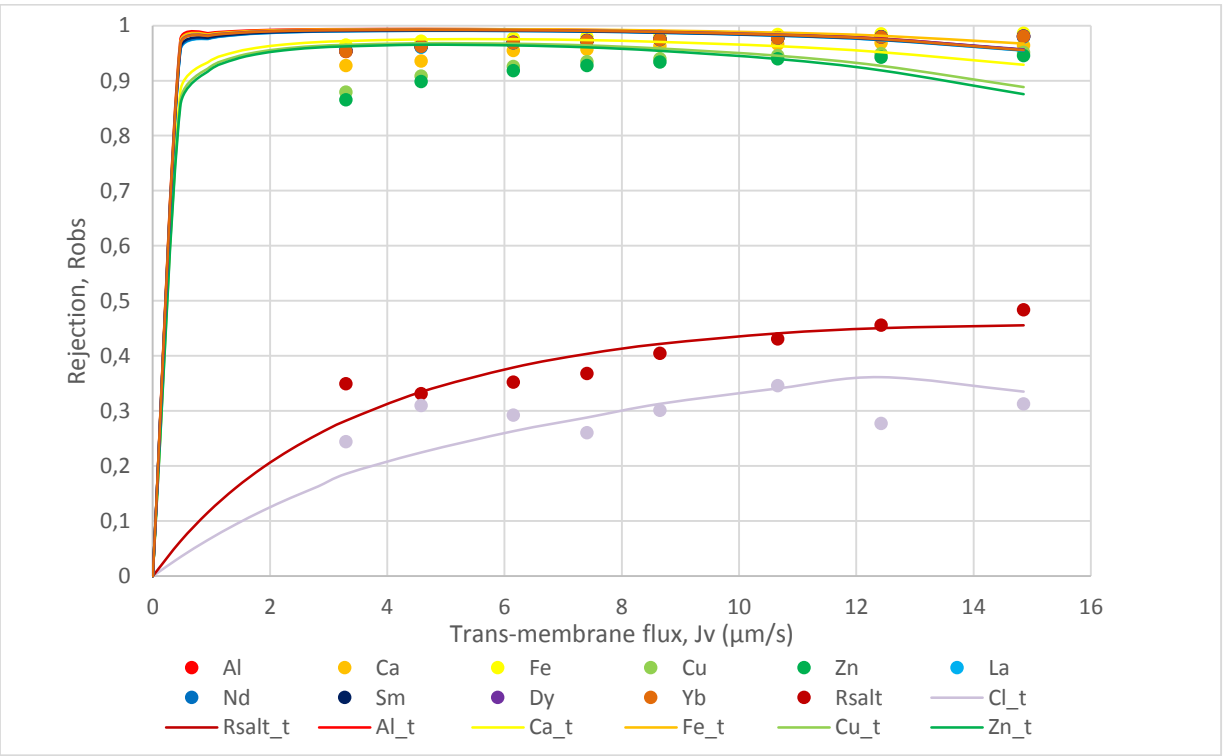

Figure 37 Results obtained with the model for the solution at pH=1 and 1500 ppm of iron

In Table 9 dominant salt and its permeabilities, as well as trace ion permeabilities can be seen.

Fe concentration (ppm)	Dominant salt	Permeability (µm/s)	
500	H_2SO_4	Al^{3+}: 0.05 H^+: 17.99 Ca^{2+}: 0.03 Fe^{3+}: 0.01 Cu^{2+}: 0.03 Zn^{2+}: 0.02 La^{3+}: 0.03	Nd^{3+}: 0.01 Sm^{3+}: 0.01 Dy^{3+}: 0.01 Yb^{3+}: 0.01 Cl^-: 12.2 SO_4^{2-}: 0.72
1000	H_2SO_4	Al^{3+}: 0.004 H^+: 8.19 Ca^{2+}: 0.02 Fe^{3+}: 0.01 Cu^{2+}: 0.04 Zn^{2+}: 0.04 La^{3+}: 0.01	Nd^{3+}: 0.01 Sm^{3+}: 0.03 Dy^{3+}: 0.01 Yb^{3+}: 0.01 Cl^-: 10.30 SO_4^{2-}: 0.72
1500	H_2SO_4	Al^{3+}: 0.01 H^+: 7.77 Ca^{2+}: 0.06 Fe^{3+}: 0.01 Cu^{2+}: 0.07 Zn^{2+}: 0.08 La^{3+}: 0.02	Nd^{3+}: 0.02 Sm^{3+}: 0.02 Dy^{3+}: 0.02 Yb^{3+}: 0.02 Cl^-: 8.38 SO_4^{2-}: 0.52

Table 10 Permeability depending on iron concentration

Next, iron permeabilities were fitted to previous equation. Figure 38 shows the results obtained.

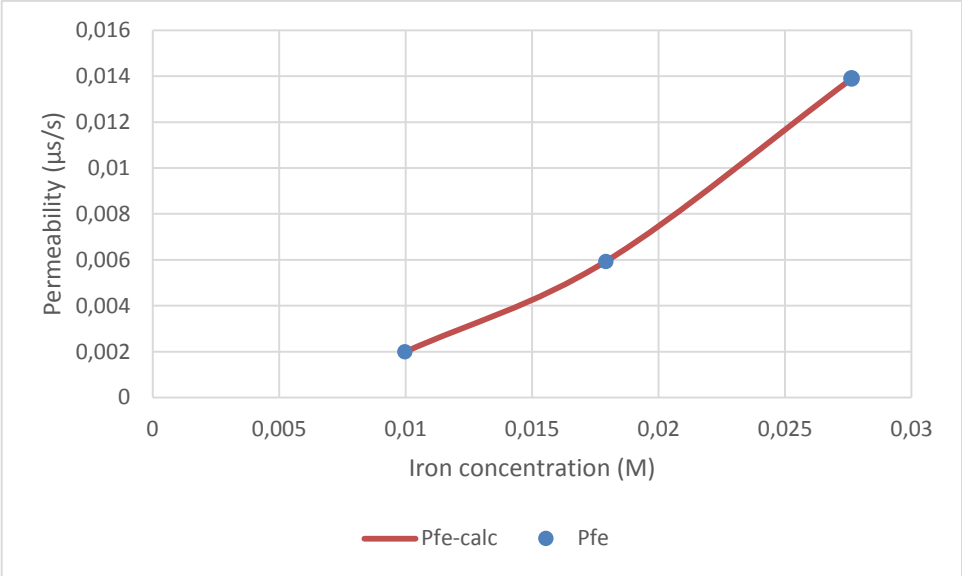

Figure 38 Iron permeability

It can be seen how permeability increases as concentration does. Values correspoding the the data modelling result almost identical to the theoretical values. Iron permeability was found to be dependent of concentration according to:

$$P_{Fe} = 19.142 \cdot C(M)^{2.02} + 0.0002 \qquad (24)$$

7.4.3 EXPERIMENTS WITH ALUMINIUM

For aluminium, experimental results are shown in Figures 39 to 42. Hydrogen was not well adjusted by the model, perhaps because of the non-ideality of the solution. It must be taken into account that pH gives a measure of hydrogen activity and not its concentration.

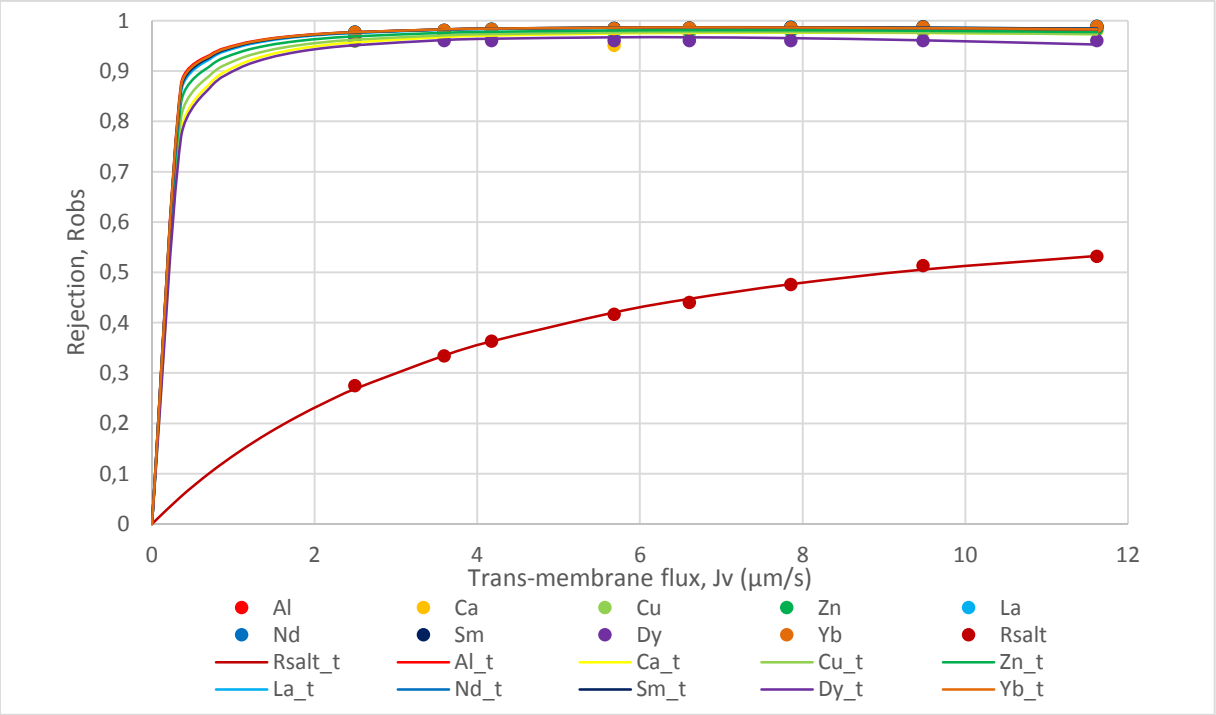

Figure 39 Results obtained with the model for the solution with pH=1 and 600 ppm of aluminium

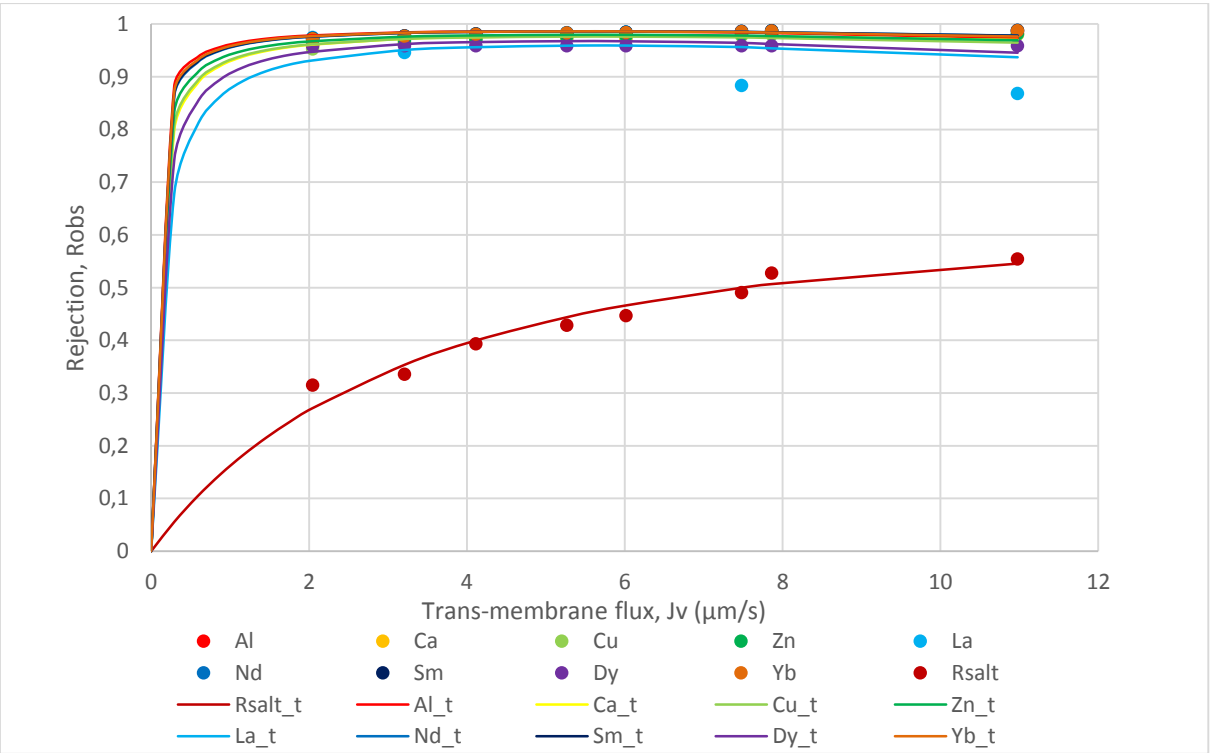

Figure 40 Results obtained with the model for the solution with pH=1 and 900 ppm of aluminium

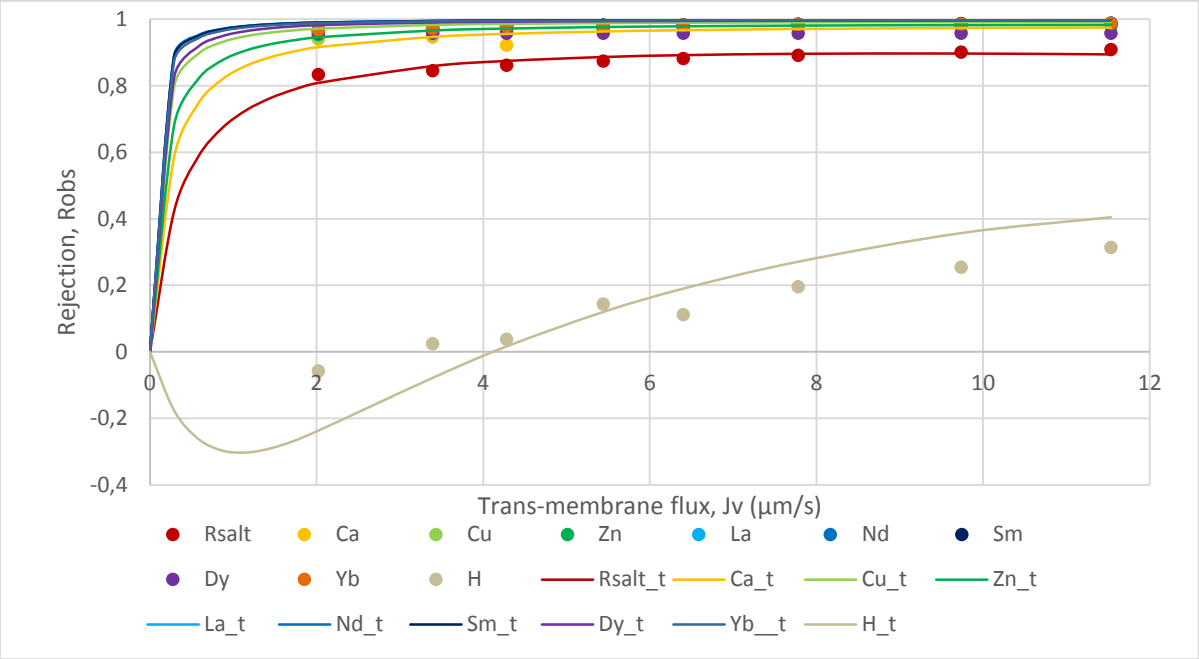

Figure 41 Results obtained with the model for the solution with pH=1 and 1200 ppm of aluminium

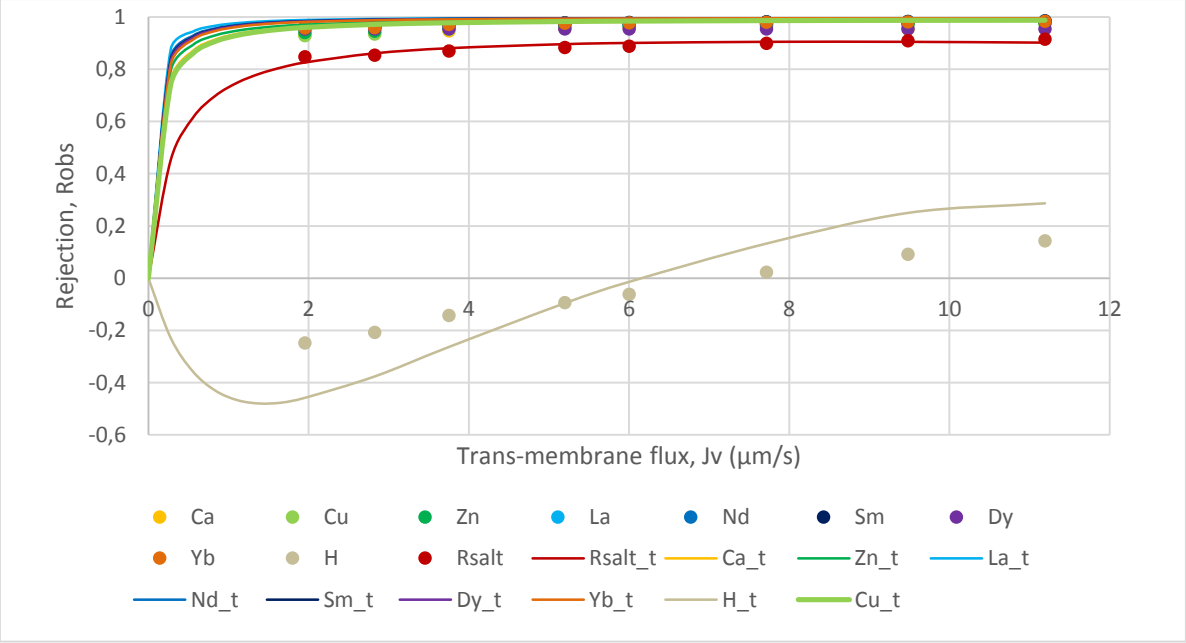

Figure 42 Results obtained with the model for the solution with pH=1 and 1500 ppm of aluminium

Next, the experiments where aluminium was added will be processed following the same procedure.

Al concentration (ppm)	Dominant salt	Permeability (μm/s)	
600	H_2SO_4	Al^{3+}: 0.05 H^+: 5.74 Ca^{2+}: 0.10 Cu^{2+}: 0.09 Zn^{2+}: 0.07 La^{3+}: 0.06	Nd^{3+}: 0.06 Sm^{3+}: 0.06 Dy^{3+}: 0.11 Yb^{3+}: 0.06 SO_4^{2-}: 0.91
900	H_2SO_4	Al^{3+}: 0.04 H^+: 4.96 Ca^{2+}: 0.08 Cu^{2+}: 0.07 Zn^{2+}: 0.06 La^{3+}: 0.15	Nd^{3+}: 0.05 Sm^{3+}: 0.05 Dy^{3+}: 0.11 Yb^{3+}: 0.04 SO_4^{2-}: 0.58
1200	$Al_2(SO_4)_3$	Al^{3+}: 0.04 Ca^{2+}: 0.47 Cu^{2+}: 0.11 Zn^{2+}: 0.24 La^{3+}: 0.06 Nd^{3+}: 0.06	Sm^{3+}:0.06 Dy^{3+}: 0.12 Yb^{3+}: 0.07 H^+: 5.49 SO_4^{2-}: 0.38
1500	$Al_2(SO_4)_3$	Al^{3+}: 0.04 Ca^{2+}: 0.15 Cu^{2+}: 0.16 Zn^{2+}: 0.11 La^{3+}: 0.07 Nd^{3+}: 0.10	Sm^{3+}: 0.11 Dy^{3+}: 0.12 Yb^{3+}: 0.13 H^+: 10.89 SO_4^{2-}: 0.32

Table 11 Permeability depending on aluminium concentration

The same graph as before will also be created, comparing experimental and theoretical values of aluminium permeability.

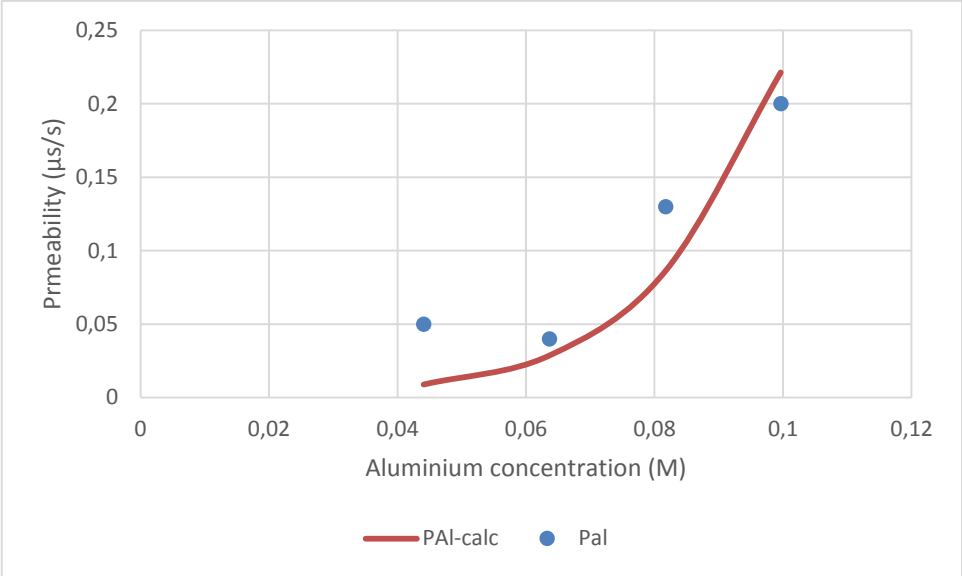

Figure 43 Aluminium permeability

There is noticeable difference between the two curves, although the tendency followed by experimental values is similar to the theoretical curve. It is observable in both graphs that it does follow the increasing tendency as more aluminium is added.

$$P_{Fe} = 19348 \cdot C(M)^{4.94} + 0.005 \quad (25)$$

8 PROJECT COSTS

In this section, the experimental costs of the project will be discussed.

First, the costs of all the salts used to prepare the solutions will be discussed.

Reagent	Quantity	Price	Cost (€)
$Al_3(SO_4)_2 \cdot 18\ H_2O$	1.12 kg	30.6 €/kg	34.27
$FeCl_3$ (30% solution)	0.43 L	18.06 €/L	7.77
$CaSO_4 \cdot 2\ H_2O$	5.6 g	50.8 €/500g	0.57
$ZnSO4 \cdot 7\ H_2O$	5.8 g	30.9 €/500g	0.90
$CuSO_4$	5.2 g	173 €/kg	0.90
$La_2(SO_4)_3 \cdot 9\ H_2O$	1.1 g	76.6 €/25g	3.37
$Pr(NO_3)_3 \cdot 6\ H_2O$	1.26 g	43.9 €/10g	5.53
$NdCl_3 \cdot 6\ H_2O$	0.94 g	75.3 €/25g	2.83
$SmCl_3$	0.92 g	272 €/10g	25.02
Dy_2O_3	0.61 g	115.5 €/25g	2.82
Yb_2O_3	0.61 g	61.2 €/10g	3.73
H_2SO_4	0.21 L	32.8 €/5L	1.38
		Total	89.09

Table 12 Cost of reagents and chemical products used

In order to carry out the experiments, two types of water were used, milli-Q and deionised water.

Water	Quantity (L)	Price (€/L)	Cost (€)
Milli-Q	2	2.8	5.6
Deionised	600	1.4	840
		Total	845.6

Table 13 Cost of water used during the experiments

Next, the costs of the membrane and the module are listed.

Equipment	Quantity	Price (€/u)	Cost (€)
Cell holder	1	5372.5	5372.5
Cell 34 Mil	1	3114	3114
Hand pump	1	825	825
O-rings	2	36	72
Spacers	2	80	160
DL membrane	2	50	100
		Total	9643.5

Table 14 Cost of the membrane and the module

Note that the price calculated for the equipment was done assuming that everything had to be bought. As all the equipment has longer expected lifetime than the duration of the experiment, costs could also be calculated correlating equipment lifetime and time that it was used.

Finally, the costs associated to the sample analysis are listed.

Analytical technique	Price (€/u)	Samples analysed	Cost (€)
ICP-MS	42.31	100	4231
ICP-OES	44.35	100	4435
		Total	8666

Table 15 Costs of sample analysis

Adding up all the costs, total experimental expenses were 19244.19 €.

9 ENVIRONMENTAL IMPACT ASSESSMENT

This section will focus on analysing the impact this project caused to the environment. The study will be limited to the laboratory plant used to carry out the experiments, and only the use of the equipment will be considered, as the plant was already built before starting this project.

Environmental impact refers to any alteration to the environment, whether good or bad, caused by human action. In this case, the objective of evaluating the impact is to identify positive and negative consequences, focusing in eliminating or reducing negative ones and maximizing positive ones.

Most of the impact caused is not significant enough, since it was a laboratory-scale plant, so, whenever possible, possible consequences of a similar industrial-scale plant will be commented.

First, it is necessary to identify the environmental aspects where this project affected the most, in this case:

Aspect	Description
Emissions and discharges	Liquid or gas substances that are disposed of into the environment
Noise pollution	Sound and vibrations produced by the equipment
Resource consumption	Consumption of electricity, fuel and water
Products and by-products	Chemical products produced by the plant
Waste	Management of waste products produced by the plant

Table 16 Environmental aspects affected by the plant

In terms of abiotic factors, the most important one is noise pollution. Upon using the pump, noise and vibrations are produced. This effect is not as significant at laboratory-scale, although it would be much more important if this project was carried out industrially, as it would play a major role while choosing the placement of the plant.

The rest of the aspects focus on treating the products produced by the plant itself. In this aspect, there are both positive and negative effects. For exemple, the discharge of chemical waste or the concentrate stream represent a negative aspect, as they pollute the environment. However, the permeate stream is a positive aspect, since metals have already been filtered and their concentrations are low, representing a positive impact to water, soil and wildlife.

Finally, there are also social and economic impacts, although they are only significant considering an industrial level plant. Generally all of these would represent positive impact, as they would include an increase in employment offer, economic expansion

and potentially higher technological development, as NF membranes are being studied. Nonetheless, negatives aspects would also exist, as energy and resources would be needed to run the plant.

Overall, this project has both positive and negative impact on the environment, although it is important to focus on the positive ones, as it provides scientific knowledge and helps improving water treatment technologies, which are benefitial for the society.

10 CONCLUSIONS

As a general conclusion, this study proved the benefits that can be provided by NF in the water treatment field, specifically reducing the environmental impact caused by AMD and the potential to separate and recover metals. This technique showed positive results in removing different ions in these types of waters, as well as being able to work at low pH. It also allows to obtain similar results to other processes, such as RO, while utilising less resources and energy. However, there is still work to be done in order to understand better NF, specifically its performance with other chemical species.

A total of 9 experiments were carried out, all with the same membrane model, 2 of them varying the pH, 3 of them adding iron, from 500 ppm to 1500 ppm, and 4 of them adding aluminium, from 600 ppm to 1500 ppm. As pH was changed, the results showed higher rejection at lower pH, except for sulphate, which showed lower rejection, as hydrogensulphate becomes more predominant, which is a monovalent ion, showing lower rejection than a divalent ion such as sulphate.

Regarding the addition of metals, as the concentration of aluminium or iron increased, rejection for all metals was slightly lower, which is also verified by the permeability graphs, as it is clear that permeability increases with the addition of iron or aluminium. The exception is sulphate rejection, which increases as metals are added. The reason is similar to the case with pH, as complexes with sulphate are formed with iron or aluminium, which results in a change from negative to positive charge, same as the membrane, which means that it is rejected better.

Finally, it was also proven that de SDFM was adequate under the experimental condition at which the experiments were carried out, as for all the samples a dominant salt could be determined and the permeability of trace ions could be determined.

Overall, NF was able to successfully treat AMD. It is clear that in future investigation, not only the acidic nature of AMD and its concentration of sulphates has to be studied, but also metals such as aluminium, iron or zinc should be considered when studying experimental solutions.

11 REFERENCES

[1] G. S. Simate and S. Ndlovu, “Acid mine drainage: Challenges and opportunities,” J. Environ. Chem. Eng., vol. 2, no. 3, pp. 1785–1803, 2014.

[2] J. Sanchez España, “Acid Mine Drainage in the Iberian Pyrite Belt : an Overview with Special Emphasis on Generation Mechanisms , Aqueous Composition and Associated Mineral Phases,” Rev. la Soc. Esp. Min., vol. 10, pp. 34–43, 2008.

[3] C. Ayora, F. Macías, E. Torres, and J. M. Nieto, “Rare Earth Elements in Acid Mine Drainage.” Environ. Sci. Technol., no. 1, pp. 1–22, 2016.

[4] X. Wei, R. C. Viadero, and K. M. Buzby, “Recovery of Iron and Aluminum from Acid Mine Drainage by Selective Precipitation,” Environ. Eng. Sci., vol. 22, no. 6, pp. 745–755, 2005.

[5] Pressure-Driven Membrane Separation Technologies [http://www.itrcweb.org/miningwaste-guidance/to_membrane_sep.htm] [11-01-17]

[6] Schäfer, A.I., Fane, A.G., Waite, “Nanofiltration: Principles and Applications.” Elsevier Science, V. 1, Ed. 1, 2004.

[7] Dach H., “Comparison of nanofiltration and reverse osmosis processes for a selective de- salination of brackish water feeds.” Université d’Angers, 2008

[8] S. A. Ahmad and S. R. Lone, “Hybrid Process (Pervaporation-Distillation): A Review,” Int. J. Sci. Eng. Res., vol. 3, no. 5, pp. 1–5, 2012.

[9] R. W. Baker, “Membrane Technology and Applications.” Ed. 2, 2004.

[10] B. Domènech, J. Bastos-Arrieta, A. Alonso, J. Macanás, M. Muñoz, and D. N. Muraviev, “Bifunctional Polymer-Metal Nanocomposite Ion Exchange Materials,” Ion Exch. Technol., no. 1 pp. 35–72., 2012.

[11] A. E. Yaroshchuk, “Dielectric exclusion of ions from membranes,” Adv. Colloid Interface Sci., vol. 85, no. 2, pp. 193–230, 2000.

[12] S. Sablani, M. Goosen, R. Al-Belushi, and M. Wilf, “Concentration polarization in ultrafiltration and reverse osmosis: A critical review,” Desalination, vol. 141, no. 3, pp. 269–289, 2001.

[13] A. W. Mohammad, Y. H. Teow, W. L. Ang, Y. T. Chung, D. L. Oatley-Radcliffe, and N. Hilal, “Nanofiltration membranes review: Recent advances and future prospects,” Desalination, vol. 356, pp. 226–254, 2015.

[14] M. Mullett, R. Fornarelli, and D. Ralph, “Nanofiltration of mine water: Impact of feed pH and membrane charge on resource recovery and water discharge,” Membranes (Basel)., vol. 4, no. 2, pp. 163–180, 2014.

[15] T. J. K. Visser, S. J. Modise, H. M. Krieg, and K. Keizer, “The removal of acid sulphate pollution by nanofiltration,” *Desalination*, vol. 140, no. 1, pp. 79–86, 2001.

[16] J. Luo and Y. Wan, “Effects of pH and salt on nanofiltration-a critical review,” J. Memb. Sci., vol. 438, pp. 18–28, 2013

[17] S. Szoke, G. Patzay, L. Weiser, “Characteristics of thin-film nanofiltration membranes at various pH-values”, Desalination 151, pp. 123–129, 2003.

[18] A. Yaroshchuk, X. Martínez-Lladó, L. Llenas, M. Rovira, J. de Pablo, J. Flores and P. Rubio, “Mechanisms of transfer of ionic solutes through composite polymer nano-filtration membranes in view of their high sulfate/chloride selectivities,” Desalination and water treatment, vol. 6, no. 1–3, pp. 48–53, 2009.

[19] A. Yaroshchuk, X. Martínez-Lladó, L. Llenas, M. Rovira, and J. de Pablo, “Solution-diffusion-film model for the description of pressure-driven trans-membrane transfer of electrolyte mixtures: One dominant salt and trace ions,” J. Memb. Sci., vol. 368, no. 1–2, pp. 192–201, 2011.

[20] A. Yaroshchuk, M. L. Bruening, and E. E. Licón Bernal, “Solution-Diffusion-Electro-Migration model and its uses for analysis of nanofiltration, pressure-retarded osmosis and forward osmosis in multi-ionic solutions,” J. Memb. Sci., vol. 447, pp. 463–476, 2013.

[21] C. Niewersch, A. L. B. Bloch, S. Yüce, T. Melin, and M. Wessling, “Nanofiltration for the recovery of phosphorus — Development of a mass transport model,” Desalination, vol. 346, pp. 70–78, 2014.

[22] J. Garcia-Aleman and J. M. Dickson, “Mathematical modeling of nanofiltration membranes with mixed electrolyte solutions,” J. Memb. Sci., vol. 235, no. 1–2, pp. 1–13, Jun. 2004.

[23] N. Fridman-Bishop, O. Nir, O. Lahav, and V. Freger, “Predicting the rejection of major seawater ions by spiral-wound nanofiltration membranes,” Environ. Sci. Technol., vol. 49, no. 14, pp. 8631–8638, 2015.

[24] A. Yaroshchuk et al., “Mechanisms of transfer of ionic solutes through composite polymer nano-filtration membranes in view of their high sulfate/chloride selectivities,” Desalin. Water Treat., vol. 6, no. 1–3, pp. 48–53, 2009.

[25] N. Pages, A. Yaroshchuk, O. Gibert, and J. L. Cortina, “Rejection of trace ionic solutes in nanofiltration : Influence of aqueous phase composition,” Chem. Eng. Sci., vol. 104, pp. 1107–1115, 2013.

[26] N. Pagès, M. Reig, O. Gibert, and J. L. Cortina, “Trace ions rejection tunning in NF by selecting solution composition: Ion permeances estimation,” Chem. Eng. J., vol. 308, pp. 126–134, 2017.

[27] P. Castro, “Eliminació d'ions trivalents d'aigües salobres mitjançant nanofiltració: Efecte de la concentració de la sal dominant.” Bachelor thesis. ETSEIB. UPC. 2015.

[28] J. B. T. Hou Xiandeng, “Inductively Coupled Plasma–Optical Emission Spectrometry,” Spectrosc. Lett., vol. 42, no. 1, pp. 58–61, 2000.

[29] A. Villegas, “Eliminació de metalls mitjançant membranes de nanofiltració: Efecte de la concentració d’alumini i ferro.” Bachelor thesis. ETSEIB. UPC. 2016.

[30] M. Reig, E. Licon, O. Gibert, A. Yaroshchuk, and J. L. Cortina, “Rejection of ammonium and nitrate from sodium chloride solutions by nanofiltration: Effect of dominant-salt concentration on the trace-ion rejection,” Chem. Eng. J., vol. 303, pp. 401–408, 2016.